Sulfonamide-based ring-fused analogues for CAN508 as novel carbonic anhydrase inhibitors endowed with antitumor activity: Design, synthesis, and *in vitro* biological evaluation

Mohamed A. Said, Wagdy M. Eldehna, Alessio Nocentini, Samar H. Fahim, Alessandro Bonardi, Abdullah A. Elgazar, Vladimír Kryštof, Dalia H. Soliman, Hatem A. Abdel-Aziz, Paola Gratteri, Sahar M. Abou-Seri, Claudiu T. Supuran

PII: S0223-5234(19)31177-8

DOI: https://doi.org/10.1016/j.ejmech.2019.112019

Reference: EJMECH 112019

To appear in: *European Journal of Medicinal Chemistry*

Received Date: 3 November 2019

Revised Date: 27 December 2019

Accepted Date: 27 December 2019

Please cite this article as: M.A. Said, W.M. Eldehna, A. Nocentini, S.H. Fahim, A. Bonardi, A.A. Elgazar, Vladimí. Kryštof, D.H. Soliman, H.A. Abdel-Aziz, P. Gratteri, S.M. Abou-Seri, C.T. Supuran, Sulfonamide-based ring-fused analogues for CAN508 as novel carbonic anhydrase inhibitors endowed with antitumor activity: Design, synthesis, and *in vitro* biological evaluation, *European Journal of Medicinal Chemistry* (2020), doi: https://doi.org/10.1016/j.ejmech.2019.112019.

Graphical Abstract

Sulfonamide-based Ring-fused analogues for CAN508 as novel carbonic anhydrase inhibitors endowed with antitumor activity: Design, synthesis, and *in vitro* biological evaluation

New sets of novel CAN508 sulfonamide-based analogues (**4**, **8a-e, 9a-h** and **10a-e**) were synthesized and evaluated for their inhibitory activity toward a panel of carbonic anhydrase isoforms hCA I, II, IX and XII, and toward CDK2 and 9. hCA IX and XII isoforms were efficiently inhibited with K_Is range of 6–67.6 and 10.1–88.6 nM, respectively. Pyrazolopyrimidines **9d**, **9e** and **10b** were found to be the most potent CDK2 inhibitors with IC_{50} = 6.4, 8.0 and 11.6 µM, respectively.

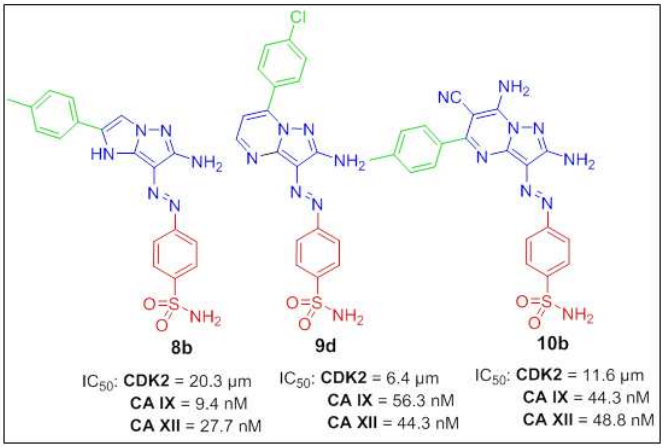

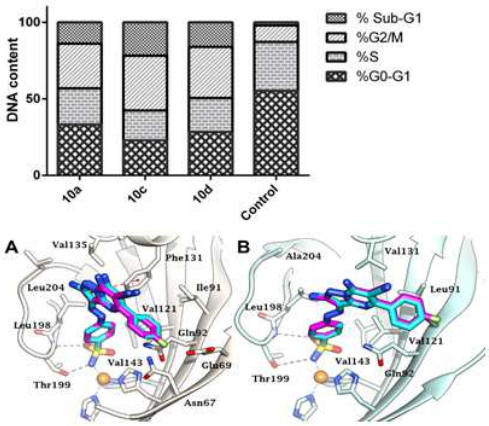

Sulfonamide-based Ring-fused analogues for CAN508 as novel carbonic anhydrase inhibitors endowed with antitumor activity: Design, synthesis, and *in vitro* biological evaluation

Mohamed A. Said[a], Wagdy M. Eldehna[b,*], Alessio Nocentini[c,d], Samar H. Fahim[e], Alessandro Bonardi[c,d], Abdullah A. Elgazar[f], Vladimír Kryštof[g], Dalia H. Soliman[a,h], Hatem A. Abdel-Aziz[i], Paola Gratteri[d], Sahar M. Abou-Seri[e,*], Claudiu T. Supuran[c,*]

[a] *Department of Pharmaceutical Chemistry, College of Pharmacy, Egyptian Russian University, Badr City, Cairo, P.O. Box 11829, Egypt*
[b] *Department of Pharmaceutical Chemistry, Faculty of Pharmacy, Kafrelsheikh University, Kafrelsheikh, P.O. Box 33516, Egypt*
[c] *Department of NEUROFARBA, Section of Pharmaceutical and Nutraceutical Sciences, University of Florence, Polo Scientifico, Via U. Schiff 6, 50019, Sesto Fiorentino, Firenze, Italy*
[d] *Department of NEUROFARBA – Pharmaceutical and nutraceutical section; Laboratory of Molecular Modeling Cheminformatics & QSAR, University of Firenze, Via U. Schiff 6, 50019 Sesto Fiorentino, Firenze, Italy*
[e] *Department of Pharmaceutical Chemistry, Faculty of Pharmacy, Cairo University, Kasr El-Aini Street, Cairo, P.O. Box 11562, Egypt*
[f] *Department of Pharmacognosy, Faculty of Pharmacy, Kafrelsheikh University, Kafrelsheikh, P.O. Box 33516, Egypt*
[g] *Laboratory of Growth Regulators, Palacky University & Institute of Experimental Botany, The Czech Academy of Sciences, Slechtitelu 27, 78371 Olomouc, Czech Republic*
[h] *Department of Pharmaceutical Chemistry, Faculty of Pharmacy, Al Azhar University, Cairo, P.O. Box 11471, Egypt*
[i] *Department of Applied Organic Chemistry, National Research Center, Dokki, Cairo 12622, Egypt*

* Corresponding authors. E-mail addresses: wagdy2000@gmail.com (W.M. Eldehna), sahar.shaarawy@pharma.cu.edu.eg (S.M. Abou-Seri), claudiu.supuran@unifi.it (C.T. Supuran).

ABSTRACT

In the present study, we report the design and synthesis of novel CAN508 sulfonamide-based analogues (**4**, **8a-e, 9a-h** and **10a-e**) as novel carbonic anhydrase (CA) inhibitors with potential CDK inhibitory activity. A bioisosteric replacement approach was adopted to replace the phenolic OH of CAN508 with a sulfamoyl group to afford compound **4**. Thereafter, a ring-fusion approach was utilized to furnish the 5/5 fused imidazopyrazoles **8a-e** which were subsequently expanded to 6/5 pyrazolopyrimidines **9a-h** and **10a-e**. All the synthesized analogues were evaluated for their inhibitory activity toward isoforms hCA I, II, IX and XII. The target tumor-associated isoforms hCA IX and XII were effectively inhibited with K_Is ranges 6–67.6 and 10.1–88.6 nM, respectively. Furthermore, all compounds were evaluated for their potential CDK2 and 9 inhibitory activities. Pyrazolopyrimidines **9d**, **9e** and **10b** displayed weak CDK2 inhibitory activity (IC_{50} = 6.4, 8.0 and 11.6 μM, respectively), along with abolished CDK9 inhibitory activity. This trend suggested that pyrazolopyrimidine derivatives merit further optimization to furnish more effective CDK2 inhibitor lead. On account of their excellent activity and selectivity towards hCA IX and XII, pyrazolopyrimidines **10** were evaluated for their anti-proliferative activity toward breast cancer MCF-7 and MDA-MB-468 cell lines under normoxic and hypoxic conditions. The most potent anti-proliferative agents **10a**, **10c** and **10d** significantly increased cell percentage at sub-G1 and G2-M phases with concomitant decrease in the S phase population in MCF-7 treated. Finally, a docking study was undertaken to investigate the binding mode for the most selective hCA IX and XII inhibitors **10a-e**, within hCA II, IX and XII active sites.

Keywords: Carbonic anhydrase inhibitors; CDK inhibitors; Molecular docking; Pyrazolopyrimidines; Imidazopyrazoles; CAN508.

1. Introduction

In spite of the significant improvement in survival among cancer patients over the last three decades [1], cancer, as described by the world health organization (WHO), is considered the second leading cause of death. It accounted for 9.6 million deaths in 2015[2]. Studies also estimate that this number is expected to double by 2030, and despite the extensive efforts and investments in this research field, it seems that the management of these human malignancies still constitute a major challenge for diagnosis and therapy. Thus, there is an ongoing need to develop new chemotherapeutic anticancer agents that may act by different mechanisms of action.

It was established that the different carbonic anhydrase (CA) isoforms are involved in numerous physiological and pathological processes all associated with CO_2 hydration reaction, such as bone resorption, calcification, electrolyte secretion, respiration, lipogenesis, gluconeogenesis, tumorigenicity and many others.[3, 4] Moreover, the hypoxia-induced *h*CA IX and XII isoforms are transmembrane tumor-associated members of the CA family. They are expressed in a limited number of normal tissues, whereas they are overexpressed in a diversity of invasive tumors such as colon, pancreas, breast, ovaries, cervix, brain, head and neck, kidney as well as lung cancers, that are associated with the hypoxic phenotype, so they are capable of affecting cell proliferation, cell adhesion and malignant cell invasion.[5, 6] Accordingly, CA isoforms IX and XII represent effective validated targets in cancer treatment strategies.

Superiorly, the zinc anchoring sulfonamides represent the most important class of the CA inhibitors, where their deprotonated form (SO_2NH^-) is coordinated to the positively charged Zn(II) ion in the enzyme active site. The “tail approach” represents the most successful approach that could be adopted to develop isoform selective CA inhibitors (CAIs). In this approach, the aromatic/heterocyclic ring possessing the sulfonamide, zinc binding group (ZBG), is appended with tail moieties through diverse functionalized linkers.[4]

Cyclin-dependent kinases (CDKs) play various essential roles in different key transitions of the cell cycle as well as in the regulation of apoptosis, neuronal functions, transcription and exocytosis.[7] Deregulation of cell cycle is accompanied by altered CDK activity in many cancers, either by activation of CDKs and/or their interacting proteins. For these reasons,

therapeutic approaches based on CDK inhibition represent a unique opportunity for drug discover and a promising strategy for treatment of human malignancies.[8, 9]

Recently, the CDK4/CDk6 inhibitors palbociclib, ribociclib and abemaciclib have received approval from the US Food and Drug Administration for the treatment of certain breast cancers and revolutionized the treatment. However, primary and acquired resistance to these drugs somehow limits the therapy and implies the necessity of development of novel therapeutic approaches [10]. Other promising CDK inhibitors in the pre/clinical development display wider kinase selectivity and anticancer potency [11]. Amongst them, purines and related heterocycles have stood out as the most investigated scaffolds for development of CDK inhibitors. Seliciclib (Roscovitine or CYC202) (**Fig. 1**) is a purine-based CDK2/ CDK7/CDK 9 inhibitor that exerts diverse effects on cell proliferation and apoptosis induction in different cancer cells. [12, 13] The success of roscovitine paved the way for further development of other CDK inhibitors, either through redistribution of nitrogen atoms of the purine nucleus such as Dinaciclib (**Fig. 1**) [14], or *via* appending different substituents to the purine scaffold such as purine-based benzenesulfonamide **I** (**Fig. 1**).[15] During our past projects, we have explored various other CDK inhibitors, where the 4-arylazo-3,5-diaminopyrazole derivatives CAN508 and AAP1742 were identified as efficient CDK2 and/ or CDK 9 inhibitors (**Fig. 1**). [9, 16, 17]

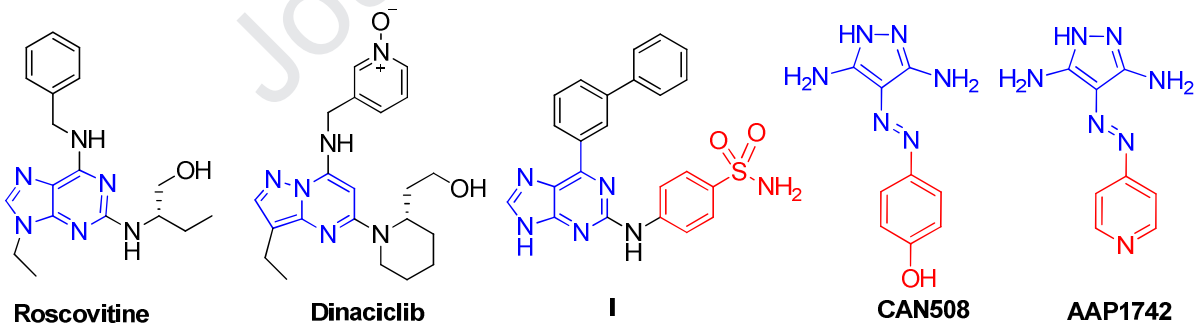

Fig. 1. Structures of some reported CDK inhibitors.

In view of the aforementioned findings and in connection with our research program in the search for effective anticancer candidates that target enzymes/proteins overexpressed in different tumors such as the tumor-associated hCA IX isoform [18-23], herein we report design and synthesis for new sets of CAN508 sulfonamide-based analogues (**4**, **8a-e, 9a-h** and **10a-e**)

with the prime aim of developing novel carbonic anhydrase inhibitors with potential CDK inhibitory activity, endowed with antitumor activity.

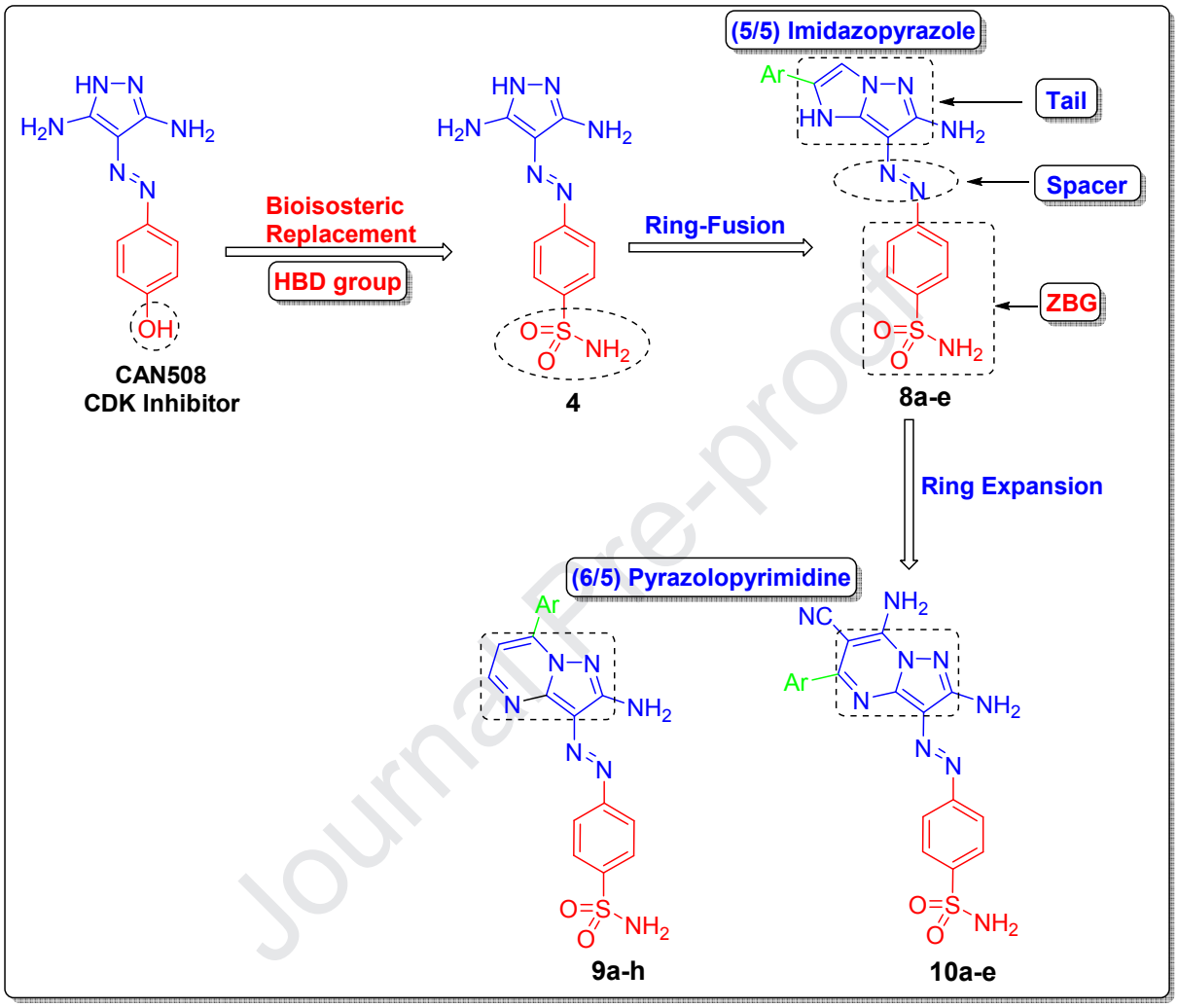

Fig. 2. Design of target sulfonamide-based ring-fused analogues for CAN508 (**4**, **8a-e, 9a-h** and **10a-e**).

Initially, the sulfamoyl group was selected to substitute the phenolic OH group of CAN508, which can interact as a H-bond donor with the side chain carboxylate of Asp145 in the CDK2 active site, in addition to the coordination of its deprotonated form (SO_2NH^-) to the positively charged Zn(II) ion in the CA active site. Thereafter, a ring-fusion approach was adopted for the pyrazole ring to furnish the 5/5 fused imidazo[1,2-*b*]pyrazole system; compounds **8a-e**. Furthermore, the imidazo[1,2-*b*]pyrazole nucleus in compounds **8** was expanded to the 6/5 fused pyrazolo[1,5-*a*]pyrimidine system to afford compounds **9a-h** and **10a-e**. Both

imidazo[1,2-*b*]pyrazole and pyrazolo[1,5-*a*]pyrimidine ring systems represent the tail for the target CAIs (**8a-e**, **9a-h** and **10a-e**). Finally, the substitution pattern on both imidazo[1,2-*b*]pyrazole and pyrazolo[1,5-*a*]pyrimidine tails was selected so as to ensure different electronic and lipophilic environments that could manipulate the potency of the target CAN508 sulfonamide-based analogues (**Fig. 2**).

All the synthesized sulfonamides were tested for their inhibitory activities toward four CA isoforms (hCA I, hCA II, hCA IX and hCA XII). Also, their inhibitory activities against CDK2 and CDK9 were assayed. In addition, compounds **8** and **10** were further evaluated against a panel of 57 human cell lines at National Cancer Institute (NCI, Bethesda, MD). Thereafter, the most selective hCA IX and XII inhibitors were examined for their anti-proliferative activity against MCF-7 and MDA-MB-468 breast cancer cell lines under normoxic and hypoxic conditions. Moreover, sulfonamides **10a**, **10c** and **10d** were assessed for cell cycle disturbance and apoptosis induction in MCF-7 cells.

2. Results and Discussion

2.1. Chemistry

The synthetic pathways employed to prepare the target CAN508 sulfonamide-based analogues (**4**, **8a-e, 9a-h** and **10a-e**) are depicted in **Schemes 1** and **2**.

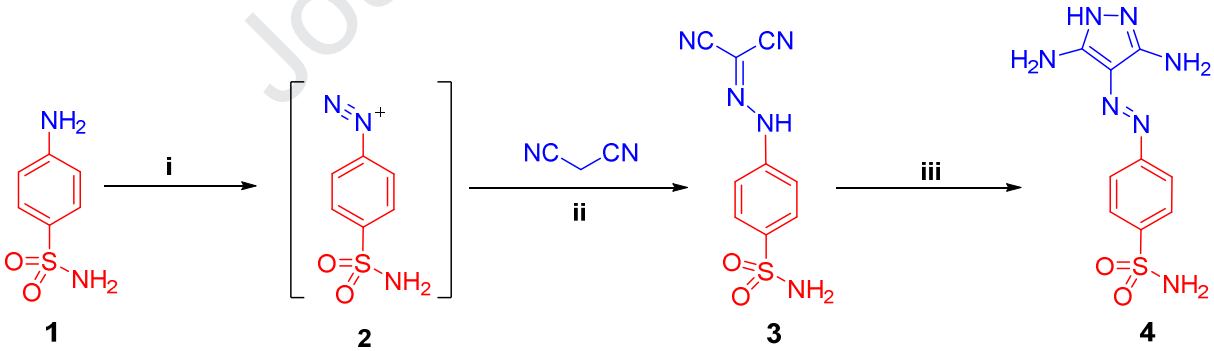

Scheme 1. Reagents and conditions: i. $NaNO_2$, HCl, 0-5 ^{0}C; **ii**. EtOH, CH_3COONa, 0-5 ^{0}C; **iii**. $NH_2NH_2.H_2O$, EtOH, reflux.

The synthesis of *N*-(4-sulfamoylphenyl)carbonohydrazonoyl dicyanide **3** was achieved by diazotization of the amino group of sulfanilamide **1**, followed by coupling the obtained diazonium with malononitrile in ethanolic sodium acetate solution at 0-5 ^{0}C as reported. [24, 25] Subsequently, preparation of (*E*)-4-((3,5-diamino-1*H*-pyrazol-4-yl)diazenyl)benzenesulfonamide

4 was carried out through refluxing the dicyanide **3** with equimolar amount of hydrazine in ethanol as described by Hassanien *et al*. [24, 26] (**Scheme 1**).

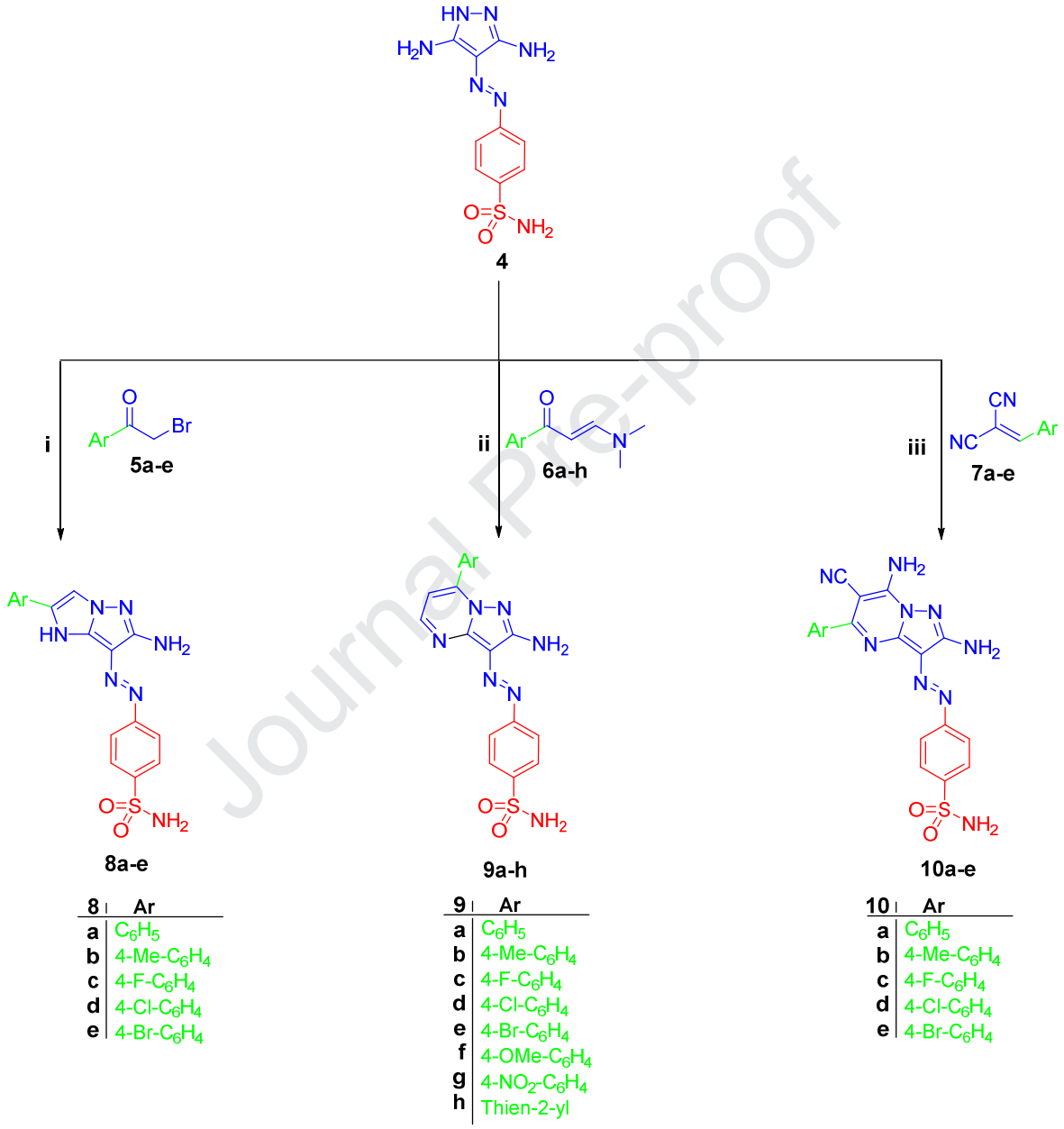

Scheme 2. Reagents and conditions: i. EtOH, DMF, reflux 12h; **ii**. AcOH, reflux 1h; **iii**. DMF, reflux 8-10h.

The diazenylbenzenesulfonamide **4** was utilized as a precursor for the synthesis of the imidazo[1,2-*b*]pyrazoles **8a-e** and the pyrazolo[1,5-*a*]pyrimidines **9a-h** and **10a-e** as shown in **Scheme 2** where three different series of reagents were required. The first series included different phenacyl bromides **5a-e** that were obtained by refluxing of appropriate acetophenone with copper (II) bromide in ethyl acetate as reported.[27, 28] The second series involved 3-(dimethylamino)-1-(aryl)prop-2-en-1-ones **6a-h** and were prepared by refluxing the corresponding acetophenone with DMF-DMA in xylene following the reported procedure.[29, 30] The third series included different benzylidenemalononitrile derivatives **7a-e** and were synthesized by heating under reflux the appropriate aldehyde with malononitrile in ethanol in presence of catalytic amount of piperidine.[31]

The target 4-((6-amino-2-(4-substitutedphenyl)-1*H*-imidazo[1,2-*b*]pyrazol-7-yl)diazenyl) benzenesulfonamides **8a-e** were obtained by reacting the key intermediate **4** with the phenacyl bromides **5a-e** in refluxing ethanol containing few drops of DMF. Alternatively, cyclocondensation of diazenylbenzenesulfonamide **4** with the appropriate arylpropinone derivative **6a-h** in glacial acetic acid or the appropriate benzylidenemalononitrile **7a-e** in DMF furnished the corresponding pyrazolo[2,3-*a*]pyrimidine **9a-h** or **10a-e**, respectively.

The IR spectra of imidazo[1,2-*b*]pyrazoles **8a-e** showed absorption bands at range of 3448-3086 cm^{-1} for the NH and two NH_2 groups, in addition to the absorption bands of SO_2 of the sulfamido group at range of 1338-1153 cm^{-1}. The ^1H NMR spectra of these compounds revealed three D_2O-exchangeable signals in the regions δ 7.34-7.41 *ppm*, 7.75-7.79 *ppm* and 11.86-11.97 *ppm* corresponding to sulfamido NH_2, 6-NH_2 and imidazole NH protons, respectively. In addition to a singlet signal in the region δ 8.44- 8.51 *ppm* assigned to the imidazo[1,2-*b*]pyrazoles H-3 proton. Compound **8b** showed additional aliphatic singlet signal corresponding to the 4-methyl substituent at δ 2.36 *ppm*. Their ^{13}C NMR spectra showed signals resonating at 110.85-164.02 *ppm* corresponding to their aromatic carbons. Compound **8b** revealed a specific signal at 21.74 *ppm* characteristic to the aliphatic carbon of its methyl group. (**Scheme 2**)

The IR spectra of pyrazolo[1,5-*a*]pyrimidines **9a-h** showed absorption bands in the range of 3437-3101 and 1334-1145 cm^{-1} due to the two NH_2 and SO_2 of the sulfamido group. The ^1H NMR spectra of **9a-h** revealed the appearance of two characteristic D_2O-exchangeable signals representing the protons of pyrazole NH_2 and sulfamido NH_2 at δ 7.40-7.57 *ppm*. Also, compounds **9b** and **9f** showed specific signals for protons of methyl and methoxy protons at δ

2.43 and 3.87 *ppm*, respectively. Moreover, ^{13}C NMR spectrum of compounds **9b** and **9f** revealed signals resonating at δ 21.57 and 55.98 *ppm* attributed to the methyl and methoxy carbons, respectively. Additionally, a high resolution mass analysis showed a molecular ion peak at 408.12357 and 428.06914 representing $[M+H]^+$ peaks of compounds **9b** and **9d**, respectively. (**Scheme 2**)

Finally, IR spectra of pyrazolo[1,5-*a*]pyrimidines **10a-e** revealed absorption bands at ranges of 3483-3066 cm^{-1} for $3NH_2$, 2210-2222 cm^{-1} for CN and 1361-1149 cm^{-1} for SO_2 of the sulfamido substituents. The ^{1}H NMR spectra of these compounds revealed the appearance of three D_2O-exchangeable signals assigned to the protons of the two amino and sulfamido NH_2 groups in the ranges of δ 7.24-7.25 *ppm*, 7.41-7.38 *ppm* and 8.64-8.71 *ppm.* Also, compound **10b** showed characteristic singlet signal at δ 2.43 *ppm* for protons of the methyl substituent, while its ^{13}C NMR spectrum revealed a signal resonating at δ 21.48 *ppm* due to the methyl carbon. HRMS spectrum of compound **10c** showed a $[M+H]^+$ peak at 452.13999 conforming its molecular weight. (**Scheme 2**)

2.2. Biological Evaluation

2.2.1. Carbonic anhydrase inhibition

All the target CAN508 sulfonamide-based analogues (**4**, **8a-e, 9a-h** and **10a-e**) were evaluated for their efficacy to inhibit the physiologically relevant hCA isoforms, hCA I and II (cytosolic) as well as hCA IX and XII (trans membrane, tumor associated isoforms) through a stopped flow CO_2 hydrase assay [32] using acetazolamide (**AAZ**) as a standard inhibitor. The following structure–activity relationship (SAR) can be concluded from the inhibition data presented in **Table 1**.

(**i**) The *in vitro* kinetic data listed in **Table 1** revealed that the ubiquitous cytosolic *h*CA I isoform was weakly inhibited by all the CAN508 ring-fused analogues reported in this study (**8a-e, 9a-h** and **10a-e**) with inhibition constants (K_Is) ranging from high nanomolar to low micromolar concentration; between 442.1 nM and 4.16 μM, apart from the non-fused analogue **4** which displayed a higher inhibitory efficacy (K_I = 270.6 nM). Noteworthy, the expanded pyrazolopyrimidine series **10** arose as the weakest *h*CA I inhibitors in this study with K_Is in the micromolar range (2.25 – 4.16 μM).

Table 1: Inhibition data of hCA isoforms I, II, IX and XII with CAN508 analogues (**4, 8a-e, 9a-h** and **10a-e**), using AAZ as a standard inhibitor.

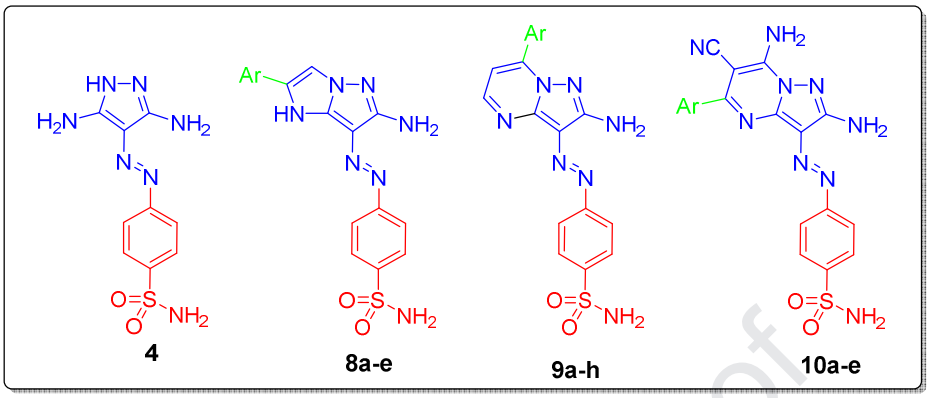

Comp.	Ar	K_I (nM)			
		hCA I	hCA II	hCA IX	hCA XII
4	-	270.6	38.1	22.0	10.1
8a	C_6H_5	957.3	75.4	38.1	30.6
8b	4-CH_3-C_6H_4	1203	99.7	9.4	27.7
8c	4-F-C_6H_4	769.3	33.8	28.4	18.6
8d	4-Cl-C_6H_4	651.3	22.1	16.6	36.5
8e	4-Br-C_6H_4	1589	49.3	44.9	52.8
9a	C_6H_5	457.9	27.6	31.8	25.4
9b	4-CH_3-C_6H_4	1331	6.2	45.7	60.7
9c	4-F-C_6H_4	681.3	14.5	6.0	31.4
9d	4-Cl-C_6H_4	543.7	23.4	56.3	44.3
9e	4-Br-C_6H_4	767.7	38.7	65.0	54.3
9f	4-OCH_3-C_6H_4	442.1	5.5	29.3	88.6
9g	4-NO_2-C_6H_4	2122	35.6	67.6	14.4
9h	2-thienyl	1154	7.1	40.1	59.0
10a	C_6H_5	2683	921.7	33.5	39.4
10b	4-CH_3-C_6H_4	3534	638.4	44.3	48.8
10c	4-F-C_6H_4	2435	398.8	8.8	10.9
10d	4-Cl-C_6H_4	2251	496.1	31.3	14.2
10e	4-Br-C_6H_4	4162	885.2	65.7	43.2
AAZ		250	12	25	5.7

* Mean from 3 different assays, by a stopped flow technique (errors were in the range of ± 5-10 % of the reported values).

(**ii**) The examined sulfonamides displayed weak to potent inhibitory activity toward the physiologically dominant off-target isoform *h*CA II (K_I values ranging between 5.5 and 921.7 nM, **Table 1**). The pyrazolopyrimidines **9b**, **9f** and **9h** emerged as the most efficient *h*CA II inhibitors with single-digit nanomolar inhibition constants (K_Is = 6.2, 5.5 and 7.1 nM, respectively). Generally, pyrazolopyrimidines **9** showed improved inhibitory profile against *h*CA II than their corresponding analogues in both imidazopyrazole **8** and pyrazolopyrimidine **10** series, except **9d** which exhibited comparable activity (K_I = 23.4 nM) to its imidazopyrazole analogue **8d** (K_I = 22.1 nM), whereas pyrazolopyrimidines **10** displayed the weakest *h*CA II inhibitory activity with K_Is in the high nanomolar range (398.8 – 921.7 μM), similar to the inhibition profile for *h*CA I.

The SAR outcomes pointed out that substitution of the pendant phenyl ring in series **8** (K_Is: 22.1 – 49.3 nM), **9** (K_Is: 5.5 – 23.4 nM) and **10** (K_Is: 398.8 – 885.2 nM) elicited an enhancement of effectiveness against hCA II in comparison to the unsubstituted analogues **8a** (K_I = 75.4 nM), **9a** (K_I = 27.6 nM) and **10a** (K_I = 921.7 nM), except for imidazopyrazole **8b** (K_I = 99.7 nM), and pyrazolopyrimidines **9e** and **9g** (K_Is = 38.7 and 35.6 nM, respectively) which displayed an elevated K_I values than their unsubstituted analogues. Moreover, bioisosteric replacement of the pendant phenyl ring in the pyrazolopyrimidine **9a** (K_I = 27.6 nM) with the heterocyclic 2-thienyl ring led to about four-fold enhanced *h*CA II inhibition potency (**9h**; K_I = 7.1 nM).

(**iii**) The *in vitro* kinetic data displayed in **Table 1** showed that the target tumor-associated hCA IX isoform was efficiently inhibited by all the CAN508 analogues herein reported. The inhibition profiles toward *h*CA IX isoform were found to be rather flat, as the measured K_I values ranged between 6.0 and 67.6 nM. Superiorly, sulfonamides **8b**, **9c** and **10c** were the most potent *h*CA IX inhibitors in this study with K_Is in a single-digit nanomolar range; 9.4, 6 and 8.8 nM, respectively.

Further analysis of the results revealed that incorporation of a small lipophilic electron-donating group on the pendant phenyl ring of imidazopyrazole series **8** (*p*-tolyl derivative **8b**; K_I = 9.4 nM) resulted in 4-fold enhanced activity compare to the unsubstituted analogues **8a** (K_I = 38.1 nM), whereas grafting the small lipophilic electron-withdrawing *p*-fluoro substituent within the two expanded pyrazolopyrimidine series **9** and **10** led to the best *h*CA IX inhibitors in this study; compounds **9c** and **10c** (K_Is = 6.0 and 8.8 nM, respectively). In contrast, incorporation of

large electron-withdrawing groups such as *p*-bromo or *p*-nitro substituents (compounds **8e**, **9e**, **9g** and **10e**; K_Is = 44.9, 65.0, 67.6 and 65.7 nM, respectively) elicited a worsening of effectiveness toward *h*CA IX in comparison to their unsubstituted counterparts **8a**, **9a** and **10a** (K_Is = 38.1, 31.8 and 33.5 nM, respectively). It is worth stressing that ring-expansion approach was more beneficial for *h*CA IX inhibitory activity in case of incorporation of unsubstituted or *p*-fluoro substituted phenyl moieties in comparison to the fused imidazopyrazole series **8**.

(**iv**) All the investigated CAN508 analogues emerged as potent inhibitors for the target tumor-associated *h*CA XII isoform (K_I values ranging between 10.1 and 88.6 nM). Interestingly, the non-fused pyrazole-based sulphonamide **4** was the most potent *h*CA XII inhibitor in this study with K_I value equals 10.1 nM. Besides, compounds **8c**, **9g**, **10c** and **10d** displayed excellent inhibitory activity toward *h*CA XII isoform (K_Is = 18.6, 14.4, 10.9 and 14.2 nM, respectively). Notably, appending the small lipophilic electron-withdrawing *p*-fluoro substituent within series **8** and **10** led to the best *h*CA XII inhibitor in each series, (compounds **8c** and **10c**; K_Is = 18.6 and 10.9 nM, respectively).

(v) Taking into account that hCA IX and XII isoforms are validated targets for treatment of human malignancies, development of selective hCA IX and XII inhibitors stands out as a crucial element to unveil an effective tumor therapy devoid of the classical side effects attributable for inhibition of the physiologically relevant off-target isoforms hCA I and II.

The calculated selectivity indexes (SIs) displayed in **Table 2** showed that all the tested compounds possessed good selectivity towards hCA IX and XII over hCA I. The results also undeniably ascribed to the pyrazolopyrimidine series **10** excellent selectivity towards hCA IX and XII over hCA I with SIs spanning in the range 63.35 – 276.70 and 68.10 – 223.39, respectively. In addition, series **10** possessed remarkable selectivity towards hCA IX and XII over hCA II with SIs ranges 13.47 – 45.32 and 13.08 – 36.59, respectively. In contrast, both series **8** and **9** failed to display a promising selectivity profile towards hCA IX and XII over hCA II regardless of their efficient inhibition of hCA IX and XII isoforms, except compound **8b** which was capable of achieving moderate selectivity over hCA II isoform.

Table 2. Selectivity index (SI) calculated for *h*CA IX and XII over off-targets isoforms (*h*CA I and II) for target sulfonamides (**8a-e, 9a-h** and **10a-e**) and **AAZ**.

Compound	Selectivity indexes			
	I\IX	**I\XII**	**II\IX**	**II\XII**
8a	25.13	31.28	1.98	2.46
8b	127.98	43.43	10.61	3.60
8c	27.09	41.36	1.19	1.82
8d	39.23	17.84	1.33	0.61
8e	35.39	30.09	1.10	0.93
9a	14.40	18.03	0.87	1.09
9b	29.12	21.93	0.14	0.10
9c	113.55	21.70	2.42	0.46
9d	9.66	12.27	0.42	0.53
9e	11.81	14.14	0.60	0.71
9f	15.09	4.99	0.19	0.06
9g	31.39	147.36	0.53	2.47
9h	28.78	19.56	0.18	0.12
10a	80.09	68.10	27.51	23.39
10b	79.77	72.42	14.41	13.08
10c	276.70	223.39	45.32	36.59
10d	71.92	158.52	15.85	34.94
10e	63.35	96.34	13.47	20.49
AAZ	10.00	43.86	0.48	2.11

2.2.2. CDK2 and 9 inhibitory activities

The newly prepared sulfonamides (**4**, **8a-e**, **9a-h** and **10a-e**) were further evaluated for their potential CDK2 and CDK9 inhibitory activity. Roscovitine and CAN508 were used as reference drugs. The results were reported as a 50% inhibition concentration values (IC_{50}), determined from triplicate dose-response curves and are listed in **Table 3**.

Results in **Table 3** revealed that only sulfonamides **9d**, **9e** and **10b** possessed weak inhibitory activity toward CDK2 (IC_{50} = 6.4, 8.0 and 11.6 μM, respectively), that is better than CAN508 (IC_{50} = 20 μM). In addition, compound **8b** displayed comparable activity (IC_{50} = 20.3 μM) to the lead CAN508 toward CDK2. In contrast, the non-fused compound **4** showed 2-fold decreased activity (IC_{50} = 41.7 μM) than CAN508 against CDK2. Unfortunately, all the

examined sulfonamides displayed non-significant inhibitory activity towards CDK9 (IC_{50} > 12.5 μM).

In summary, the adopted bioisosteric replacement of the phenolic group of CAN508 with a sulfamoyl group resulted in 2-fold decreased potency toward CDK2 (compound **4**; IC_{50} = 41.7 μM), whereas, the ring fusion approach just maintained the CDK2 inhibitory activity (imidazopyrazole **8b**; IC_{50} = 20.3 μM). On the other hand, the ring expansion approach successfully enhanced the inhibitory activity towards CDK2, such pyrazolopyrimidines **9d**, **9e** and **10b** (IC_{50} = 6.4, 8.0 and 11.6 μM, respectively). Interestingly, increased potency against CDK2 was accompanied with an abolished activity towards CDK9. Accordingly, this trend of activity pointed out that the herein reported pyrazolopyrimidine-based CDKIs merit further optimization and development to furnish more promising selective CDK2 inhibitors.

Table 3. IC_{50} values for the inhibitory activity of **4, 8a-e, 9a-h and 10a-e** against CDK2 and 9.

Compound	IC_{50} (μM)	
	CDK2	**CDK9**
4	**41.7**	>12.5
8a	>25	>25
8b	**20.3**	>12.5
8c	>12.5	>12.5
8d	>12.5	>12.5
8e	>12.5	>12.5
9a	>12.5	>12.5
9b	>12.5	>12.5
9c	>12.5	>12.5
9d	**6.4**	>12.5
9e	**8.0**	>12.5
9f	>12.5	>12.5
9g	>12.5	>12.5
9h	>12.5	>12.5
10a	>12.5	>12.5
10b	**11.6**	>12.5
10c	>12.5	>12.5
10d	>12.5	>12.5
10e	>12.5	>12.5
CAN508	20	0.35
Roscovitine	0.1	1.8

2.2.3. Anticancer Activity

2.2.3.1. NCI antitumor activity screening

Sulfonamides (**8a-e** and **10a-e**) were selected to be examined for their antitumor activity at the NCI-Developmental Therapeutic Program (www.dtp.nci.nih.gov). They were screened in a primary one dose (10 μM) anticancer assay against a panel of 57 cancer cell lines, in accordance with the protocol of the Drug Evaluation Branch, NCI, Bethesda [33]. The data are reported as mean-graph of the percent growth of the treated cancer cells and presented, in **Table 4**, as percentage growth inhibition (GI%) caused by the examined sulfonamides.

Investigation of the obtained data in **Table 4** revealed that the examined CAN508 sulfonamide-based analogues exhibited distinctive patterns of sensitivity and selectivity toward the different cancer cell panels. Inspecting the GI% values, pointed out that Imidazopyrazole derivative **8a** stood out as the most potent CAN508 analogue in this study with mean GI = 68%. It exhibited broad spectrum anticancer activity against all the tested cancer cell lines with an exception to ovarian (NCI/ADR-RES) cancer cell line. Superiorly, sulfonamide **8a** displayed an excellent growth inhibitory activity against Leukemia (MOLT-4, RPMI-8226 and SR), CNS (SNB-75), ovarian (IGROV1 and SK-OV-3), Renal (A498, ACHN, CAKI-1 and RXF 393), and breast cancer (HS 578T) cell lines with GI% range = 85- 96. In addition, sulfonamide **8a** displayed potent GI more than 75% toward Leukemia (CCRF-CEM), Non-small cell lung cancer (NCI-H460), colon cancer (HCT-116 and HCT-15), CNS (SF-539), Melanoma (LOX IMVI), Renal (SN12C and UO-31), and breast cancer (MDA-MB-231/ATCC) cell lines, **Table 4**.

Moreover, pyrazolopyrimidine **10b** was found to be the second most potent analogue (mean GI% = 61) with broad spectrum activity against all the tested cancer cell lines, except Ovarian (NCI/ADR-RES) cancer cell line. **10b** exerted outstanding anti-proliferative activity against Leukemia (CCRF-CEM, HL-60TB, K-562 and MOLT-4), Non-small cell lung cancer (HOP-92), Colon cancer (COLO 205, HCT-116 and SW-620), Renal (ACHN) and Breast (MDA-MB-468) cell lines with GI% ranging from 80 to 100 %, **Table 4**. Furthermore, sulfonamides **8b**, **8e** and **10e** (mean GI = 50, 46 and 50%, respectively) displayed promising broad spectrum growth inhibitory activity towards most of the tested cancer cell lines.

Table 4. Percentage growth inhibition (GI %) of *in vitro* subpanel tumor cell lines at 10 μM concentration for sulfonamides **8a-e** and **10a-e**.

Subpanel/ Cell line		Compound [a]									
		8a	**8b**	**8c**	**8d**	**8e**	**10a**	**10b**	**10c**	**10d**	**10e**
Leukemia	**CCRF-CEM**	80	54	33	----	45	21	88	51	65	104
	HL-60(TB)	72	47	----	----	36	----	97	----	----	62
	K-562	67	48	----	----	38	----	80	33	28	64
	MOLT-4	86	55	----	----	42	----	96	62	82	98
	RPMI-8226	94	60	27	----	55	----	116	60	58	114
	SR	87	63	33	28	54	----	71	----	----	59
Non-Small Cell Lung Cancer	**A549/ATCC**	67	62	----	----	51	----	37	----	----	32
	EKVX	45	28	----	----	21	----	30	----	----	29
	HOP-62	58	39	----	----	37	----	57	21	24	48
	HOP-92	74	35	25	----	29	27	80	58	29	69
	NCI-H226	47	27	----	----	----	24	35	25	25	34
	NCI-H23	54	34	----	----	30	----	56	----	----	36
	NCI-H322M	63	69	58	25	65	21	34	21	----	25
	NCI-H460	80	67	41	25	62	----	72	----	21	63
	NCI-H522	69	57	45	30	55	54	71	32	29	61
Colon Cancer	**COLO 205**	55	24	----	----	28	----	86	----	----	74
	HCC-2998	54	40	----	----	33	----	48	----	----	38
	HCT-116	77	62	37	----	62	----	86	24	34	75
	HCT-15	77	65	40	----	63	----	18	----	----	----
	HT29	61	37	----	----	34	----	64	----	----	57
	KM12	67	46	27	----	39	50	71	53	75	48
	SW-620	74	60	23	----	48	----	83	----	----	56
CNS Cancer	**SF-268**	63	49	23	----	42	----	65	----	23	44
	SF-295	52	29	----	----	----	----	51	----	----	38
	SF-539	80	56	27	----	42	----	69	28	25	61
	SNB-19	40	24	----	----	26	----	42	----	----	38
	SNB-75	99	66	44	23	64	----	51	33	----	43
	U251	61	44	24	----	38	----	68	28	30	59
Melanoma	**LOX IMVI**	83	70	36	21	64	----	78	28	----	71
	MALME-3M	74	63	42	----	64	----	51	20	----	42
	M14	69	60	35	21	61	----	54	----	----	59
	MDA-MB-435	71	52	22	----	46	----	48	----	----	44
	SK-MEL-2	68	57	30	----	53	----	73	25	24	57
	SK-MEL-28	55	38	----	----	32	----	47	----	----	37

	SK-MEL-5	73	51	23	----	45	----	152	31	31	54
	UACC-257	31	20	----	----	21	----	28	----	----	----
	UACC-62	69	44	29	----	47	----	47	----	----	28
Ovarian Cancer	**IGROV1**	85	80	38	21	72	35	63	36	----	59
	OVCAR-3	53	36	21	----	27	----	76	20	25	45
	OVCAR-4	63	46	----	----	43	----	48	----	----	39
	OVCAR-5	35	23	----	----	24	----	21	----	----	28
	OVCAR-8	63	47	21	----	37	----	56	25	25	53
	NCI/ADR-RES	----	----	----	----	----	----	----	----	----	----
	SK-OV-3	87	77	26	21	82	----	36	----	----	----
Renal Cancer	**786-0**	72	60	32	28	56	----	35	----	----	30
	A498	92	87	60	65	83	30	41	----	----	35
	ACHN	91	79	48	29	76	----	100	----	----	29
	CAKI-1	96	86	53	35	82	----	59	----	26	47
	RXF 393	93	56	40	29	55	42	72	59	29	58
	SN12C	80	63	31	----	58	24	67	24	27	54
	TK-10	52	53	----	27	50	----	34	----	----	27
	UO-31	81	77	42	22	74	25	31	38	36	41
Prostate	**PC-3**	68	43	----	----	39	----	68	29	38	62
	DU-145	57	52	30	----	47	----	65	----	40	67
Breast Cancer	**MCF7**	54	----	----	----	33	60	72	59	51	68
	MDA-MB-231/ATCC	80	42	25	----	43	----	60	37	52	59
	HS 578T	95	64	33	21	54	----	61	23	30	55
	BT-549	41	33	26	34	25	----	44	----	35	26
	T-47D	57	39	22	----	46	26	66	48	56	68
	MDA-MB-468	67	48	----	----	51	58	94	71	56	76
Mean growth, %		68	50	25	14	46	12	61	22	22	50
Sensitive cell lines no.		59	58	38	18	57	14	59	30	30	56

[a] Only GI % higher than 20% are shown.

Regarding sensitivity of individual cell lines (Table 4), only Non-small cell lung cancer (NCI-H522) and Renal (RXF 393 and UO-31) cancer cell lines were susceptible to all the examined CAN508 analogues (**8a-e** and **10a-e**), whereas, the Ovarian NCI/ADR-RES cancer cell line uniquely hasn't been affected by any of the examined compounds. Notably, sulfonamides **10b** and **10e** exerted cytotoxic effect with GI more than 100% toward certain cancer cell lines.

Sulfonamide **10b** was proved to be lethal to Leukemia RPMI-8226 and Melanoma SK-MEL-5 cell lines (GI % = 116 and 152, respectively), whereas, sulfonamide **10e** exerted its lethal activity toward Leukemia CCRF-CEM cell line with GI %=114, Table 4.

2.2.3.2. In vitro anti-proliferative activity

While, both imidazopyrazoles **8** and pyrazolopyrimidines **10** exhibited significant growth inhibitory activities in 57 cancer cell lines-NCI screening assay, only the pyrazolopyrimidine derivatives **10a-e** displayed good selectivity towards tumor associated isoform hCA IX over hCA I (SI: 63.35 – 276.70) and hCA II (SI: 13.47 – 45.31), in addition to their good inhibitory activities towards both hCA IX and XII isoforms (K_Is: of 8.8 – 65.7 and 10.9 – 48.8 nM, respectively). Accordingly, compounds **10a-e** were selected to be evaluated for their anti-proliferative activity against two breast cancer cell lines overexpressing CA IX, namely MCF-7 and MDA-MB-468 cell lines [34], using MTT assay [35]. Notably, both breast cancer cell lines were proved to be susceptible to the influence of compounds **10a-e** in the NCI screening assay. In this assay, cobalt (II) chloride ($CoCl_2$) was utilized as an inducer of HIF-1α to furnish a chemically-induced hypoxia [36] in order to further evaluate the antiproliferative activity of **10a-e** under hypoxic conditions. Staurosporine, a clinically used anticancer drug, was co-assayed as a reference drug. The results are expressed as IC_{50} values and displayed in **Table 5**.

Table 5. *In vitro* anti-proliferative activity of pyrazolopyrimidines **10a-e** against breast MCF-7 and MDA-MB-468 cancer cell lines under normoxic and hypoxic conditions.

Compound	IC_{50} (μM)[a]			
	MCF-7		MDA-MB-468	
	Normoxia	Hypoxia	Normoxia	Hypoxia
10a	0.66±0.03	0.96±0.04	1.89±0.04	1.07±0.05
10b	6.80±0.17	15.10±0.82	1.37±0.07	3.03±0.11
10c	2.96±0.06	7.73±0.26	5.38±0.16	11.30±0.74
10d	2.07±0.08	10.30±0.75	11.44±0.76	19.61±1.42
10e	4.77±0.08	7.56±0.33	6.81±0.28	10.02±0.84
Staurosporine	3.39±0.13	9.20±0.41	4.37±0.17	6.46±0.26

a. IC_{50} values are the mean ± S.D. of three separate experiments.

Exploring the results of the MTT assay highlighted that the tested sulfonamides **10a-e** showed potent to good inhibitory activity against both cell lines under the tested normoxic and hypoxic conditions. The tested compounds were more effective toward MCF-7 cells than MDA-MB-468 cells, except sulfonamide **10b** which displayed much enhanced growth inhibitory activity, under normoxic and hypoxic conditions, against MDA-MB-468 (IC_{50} = 1.37±0.07 and 3.03±0.11 µM) than MCF-7 cells (IC_{50} = 6.80±0.17 and 15.10±0.82 µM). Concerning the anti-proliferative activity towards MCF-7 cells, sulfonamide **10a** (IC_{50} = 0.66±0.03 and 0.96±0.04 µM, under normoxic and hypoxic conditions, respectively) was found to be the most active analogue in this study, being 5- and 9-times more potent than reference drug staurosporine (IC_{50} = 3.39±0.13 and 9.20±0.41 µM, under normoxic and hypoxic conditions, respectively). Also, compounds **10c** and **10d** displayed higher or comparable anti-proliferative activities to staurosporine, with IC_{50} values equal 2.96±0.06 and 2.07±0.08 µM, respectively, for normoxic condition, and 7.73±0.26 and 10.30±0.75 µM, respectively, for hypoxic condition.

On the other hand, exploring the growth inhibitory activity of sulfonamides **10a-e** against MDA-MB-468 cells revealed that sulfonamides **10a** and **10b** were the most effective counterparts (IC_{50} = 1.89±0.04 and 1.37±0.07 µM, respectively for normoxic condition, and 1.07±0.05 and 3.03±0.11 µM, respectively, for hypoxic condition), with 2.3- and 3.1-fold enhanced efficiency under normoxic condition, and 6- and 2.1-fold enhanced efficiency under hypoxic condition, than staurosporine (IC_{50} = 4.37±0.17 and 6.46±0.26 µM, under normoxic and hypoxic conditions, respectively).

2.2.3.3. Cell Cycle Analysis

To acquire mechanistic insights into the anti-proliferative activity of the target sulfonamides, compounds **10a**, **10c** and **10d** were assessed for their impact on the cell cycle distribution in MCF-7 cells through a DNA flow cytometric assay (**Fig. 3**). The outcomes of this flow cytometric assay highlighted that treatment of MCF-7 cells with sulfonamides **10a**, **10c** and **10d** at their IC_{50} concentrations (0.66, 2.96 and 2.07 µM) induced a significant cell cycle arrest at G_2-M phase and decreased the S-phase populations with subsequent increase in the percentages apoptotic cells at Sub-G_1 phase by 7, 11 and 8-fold compared to the control, respectively.

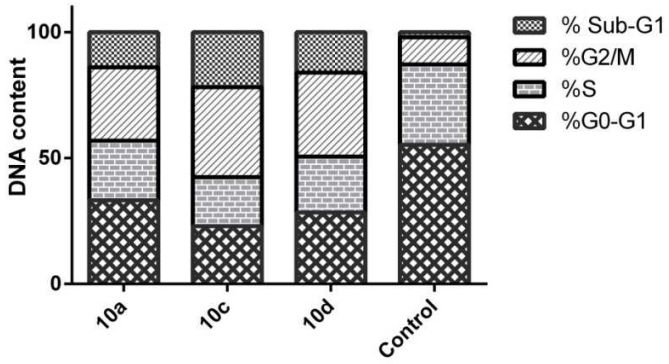

Figure 3. Effect of sulfonamides **10a**, **10c** and **10d** on the phases of cell cycle of MCF-7 cells.

2.2.3.4. Annexin V-FITC Apoptosis Assay

To investigate whether the anti-proliferative activities of target sulfonamides **10** is consistent with the apoptosis induction within the breast cancer MCF-7 cells suggested by the presence of sub-G1 population of treated cells (**Fig. 3**), Annexin V-FITC/propidium iodide dual staining assay (AV/PI) was carried out by flow cytometry (**Fig. 4**, **Table 6**).

The obtained results suggested that sulfonamides **10a**, **10c** and **10d** have the ability to persuade the apoptosis in MCF-7 cells as evidenced by the significant increase in the percent of annexin V-FITC-positive apoptotic cells, including both the early (from 0.47% to 8.46% (**10a**), 6.58% (**10c**), and 5.88% (**10d**)) and late apoptosis (from 0.29% to 16.94% (**10a**), 10.89% (**10c**), and 8.2% (**10d**)) phases, which represents about 26-, 23- and 18-fold total increase as compared with the untreated control (**Fig. 4**, **Table 6**).

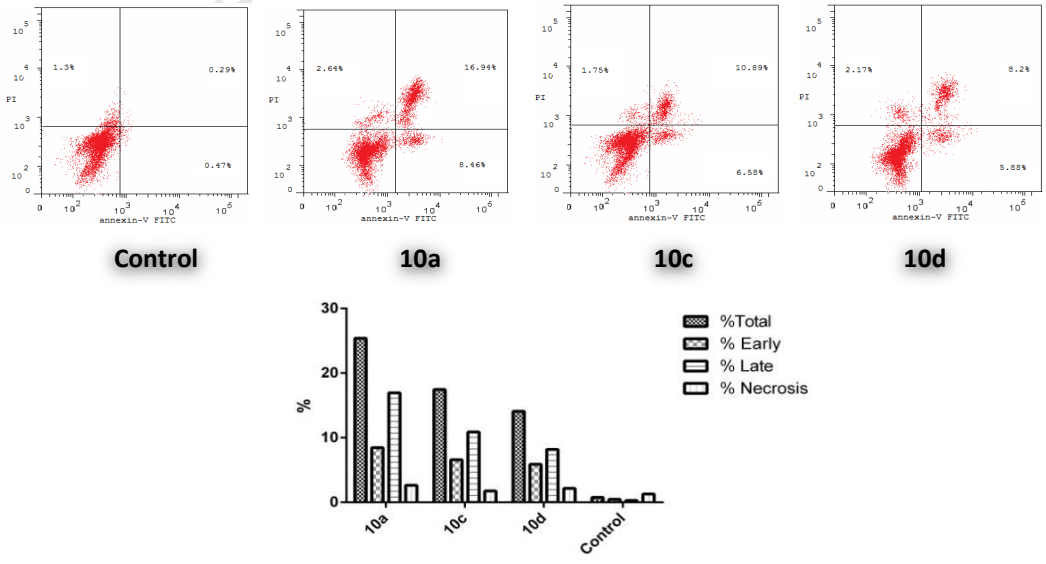

Fig. 4. Effect of sulfonamides **10a**, **10c** and **10d** on the percentage of annexin V-FITC-positive staining in breast cancer MCF-7 cells. The experiments were done in triplicates. The four quadrants identified as: LL, viable; LR, early apoptotic; UR, late apoptotic; UL, necrotic.

2.2.4. Computational studies

Docking studies were undertaken to investigate the binding mode and point out the relationships between the inhibition profile and structural features for the most selective compounds of the series, **10a-e**, within hCA II (pdb 5LJT [37]), IX (pdb 5FL4 [38]) and XII (pdb JLD0 [39]). In all docking solutions, the benzenesulfonamide moiety accommodates deeply into the active site of the three isozymes (**Fig. 5**). In particular, the sulfonamide coordinates to the zinc ion through the negatively charged nitrogen and also engages two H-bonds, occurring between the NH^- and the S=O groups of the ligand and Thr199 (N-H···OG1 and S=O···H-N). The placement of phenyl ring is stabilized by hydrophobic interactions with residues Val121, Val143, and Leu198.

Within the binding site of the tumor-associated CAs, the 5-phenylpyrazolopyrimidine moiety of the ligands adopts an orientation whereby intense interactions of the hydrophobic type occur with the pocket lined by Leu91, Gln92, Val121 and Val131 in CA IX (**Fig. 5B**) and Thr91, Gln92, Val121 and Ala131 in CA XII (**Fig. 5C**).

As it often occurs with bulky and rigid pendants at the benzenesulfonamide scaffold, the Phe131/Val131 (CA II/IX) and Phe131/Ala131 (CA II/XII) induces a different placement for the ligand tail within the active site of the ubiquitous isozyme, which prevents strong contacts with the hydrophobic cleft of the binding cavity and drives the terminal phenyl moiety toward the hydrophilic area (**Fig. 5A**). This could explain the **10a-e** better efficacy against the cancer-related CAs over CA II. The 4-substitution of the outer phenyl ring did not influence the heterocycle binding orientation within the three active sites (**Fig. 5**).

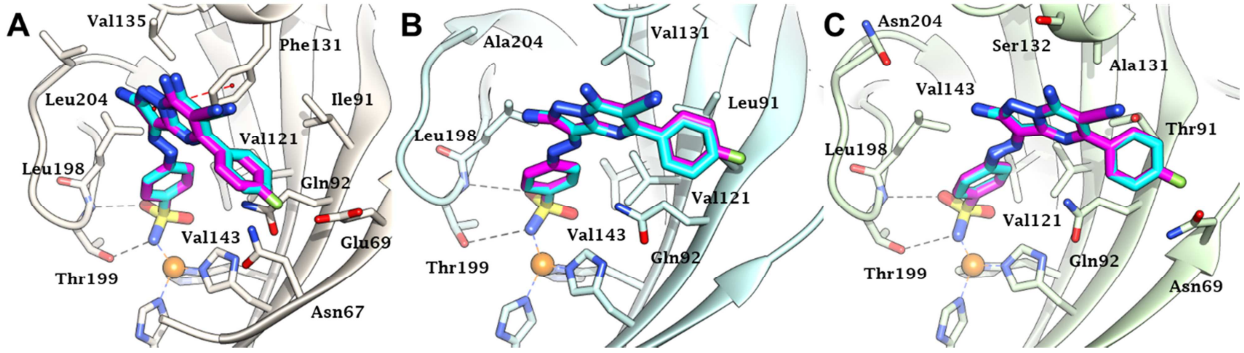

Figure 5: Binding mode of **10a** (cyano) and **10c** (magenta) within A) hCA II, B) hCA IX and C) hCA XII active sites.

3. Conclusion

In summary, herein we described the design and synthesis of new sets of novel CAN508 sulfonamide-based analogues (**4**, **8a-e, 9a-h** and **10a-e**) as novel carbonic anhydrase (CA) with potential CDK inhibitory activity. A bioisosteric replacement approach was adopted to replace the H-bond donor phenolic OH of CAN508 with a sulfamoyl group to afford compound **4**. Thereafter, a ring-fusion approach was utilized to furnish the 5/5 fused imidazopyrazoles **8a-e** which subsequently expanded to 6/5 pyrazolopyrimidines **9a-h** and **10a-e**. All the synthesized analogues were evaluated for their inhibitory activity towards a panel of CA isoforms hCA I, II, IX and XII. The target tumor-associated isoforms hCA IX and XII were effectively inhibited with K_Is ranges 6–67.6 and 10.1–88.6 nM, respectively. In particular, sulfonamides **8b**, **9c** and **10c** were the most potent *h*CA IX inhibitors in this study with K_Is in a single-digit nanomolar range; 9.4, 6 and 8.8 nM, respectively. The obtained inhibition profiles ascribed to pyrazolopyrimidine series **10** excellent selectivity towards hCA IX and XII over hCA I (SIs: 63.35 – 276.70 and 68.10 – 223.39, respectively) and over hCA II (SIs: 13.47 – 45.32 and 13.08 – 36.59, respectively). Furthermore, all compounds were evaluated for their potential CDK2 and 9 inhibitory activities. Pyrazolopyrimidines **9d**, **9e** and **10b** displayed weak CDK2 inhibitory activity (IC_{50} = 6.4, 8.0 and 11.6 μM, respectively), along with abolished CDK9 inhibitory activity. On account of their excellent activity and selectivity towards hCA IX and XII, pyrazolopyrimidines **10** were evaluated for their anti-proliferative activity toward breast cancer MCF-7 and MDA-MB-468 cell lines under normoxic and hypoxic conditions. As compounds **10a**, **10c** and **10d** emerged as the most potent anti-proliferative agents against MCF-7 cells, they

were selected to be assessed for their impact on the cell cycle distribution and apoptotic potential in MCF-7 cells. They disrupted the MCF-7 cell cycle *via* alteration of the Sub-G_1 phase and arrest of G_2-M stage, and displayed significant increase in the percent of annexinV-FITC positive apoptotic cells. Finally, a docking study was carried out to investigate the binding modes and to justify the selectivity of series **10** toward isoforms hCA IX and XII over hCA II. It was suggested that the Phe131/Val131 (CA II/IX) and Phe131/Ala131 (CA II/XII) induced a different placement for the bulky and rigid pyrazolopyrimidine tail within the active site of the ubiquitous isozyme, which could prevent strong contacts with the hydrophobic cleft of the binding cavity, and drives the terminal phenyl moiety toward the hydrophilic area.

4. Experimental

4.1. Chemistry

4.1.1. General

Melting points were measured with a Stuart melting point apparatus and were uncorrected. Infrared spectra were recorded on Schimadzu FT-IR 8400S spectrophotometer. The NMR spectra were recorded by Bruker spectrometer at 400 MHz. 13C NMR spectra were run at 100 MHz in deuterated dimethylsulfoxide (DMSO-*d6*). Chemical shifts (δ_H) are reported relative to the solvent (DMSO-d_6). All coupling constant (J) values are given in hertz. Chemical shifts (δ_C) are reported relative to the solvent (DMSO-d_6). High-resolution mass spectra were recorded using a Bruker MicroTOF spectrometer. Elemental analyses were carried out at the Regional Center for Microbiology and Biotechnology, Al-Azhar University, Cairo, Egypt. Unless otherwise noted, all solvents and reagents were commercially available and used without further purification. Compounds (**3**) [24, 25], (**4**) [25, 26], (**5a-e**) [27, 28], (**6a-h**) [29, 30] and (**7a-e**) [31] were synthesized as reported previously.

4.1.2. *Synthesis of 4-((6-amino-2-(4-substitutedphenyl)-1H-imidazo[1,2-b]pyrazol-7-yl)diazenyl)benzenesulfonamide (**8a-e**)*

The key intermediate **4** (7 g, 0.02 mol) was added to a preheated, stirred suspension of **5a-e** (0.05 mol) in absolute ethanol (25 mL) and few drops of DMF. The resulting reaction mixture was heated under reflux for 12h with stirring. Then reaction mixture was filtered while hot, and

the obtained solid was washed with hot ethanol and recrystallized from DMF/ethanol to afford the target compounds **8a-e**.

4.1.2.1. 4-((6-Amino-2-phenyl-1*H*-imidazo[1,2-*b*]pyrazol-7-yl)diazenyl)benzenesulfonamide (**8a**)

Yield (45%); brick red powder; m.p. >300 °C; IR: 3402, 3313, 3240, 3174, 3155 (NH, $2NH_2$), 1338, 1153 (SO_2); ^{1}H NMR *δ ppm*: 7.37 (br s, 2H, -SO_2NH_2), 7.43 (t, 1H, Ar-H, *J* = 7.2 Hz), 7.54 (t, 2H, Ar-H, *J* = 7.6 Hz), 7.76 (br s, 2H, -NH_2 of pyrazole), 7.88 (d, 2H, Ar-H, *J* = 8.8 Hz), 7.95 (d, 2H, Ar-H, *J* = 8.0 Hz), 8.01 (d, 2H, Ar-H, *J* = 8.8 Hz), 8.51 (s, 1H, Ar-H), 11.97 (br s, 1H, -NH); ^{13}C NMR *δ ppm*: 110.85, 115.51, 120.29, 125.06, 127.85, 129.21, 129.73, 130.78, 138.45, 138.76, 145.32, 153.86, 162.14; MS *m/z* %: 381.4 (M^+, 19.12); Anal. Calcd. for $C_{17}H_{15}N_7O_2S$: C, 53.53; H, 3.96; N, 25.71; found C, 53.71; H, 3.92; N, 25.75.

4.1.2.2. 4-((6-Amino-2-(4-methylphenyl)-1*H*-imidazo[1,2-*b*]pyrazol-7-yl)diazenyl)benzenesulfonamide (**8b**)

Yield (39%); brick red powder; m.p. >300 °C; IR: 3390, 3309, 3240, 3174 (NH, $2NH_2$), 1334, 1153 (SO_2); ^{1}H NMR *δ ppm*: 2.36 (s, 3H, CH_3), 7.34-7.36 (m, 4H, 2H, -SO_2NH_2 and 2H, Ar-H), 7.75 (br s, 2H, -NH_2 of pyrazole), 7.82 (d, 2H, Ar-H, *J* = 8.0 Hz), 7.88 (d, 2H, Ar-H, *J* = 8.4 Hz), 8.01 (d, 2H, Ar-H, *J* = 8.4 Hz), 8.44 (s, 1H, Ar-H), 11.86 (br s, 1H, -NH); ^{13}C NMR *δ ppm*: 21.74 (CH_3), 110.67, 115.24, 121.11, 124.98, 127.09, 128.65, 129.94, 132.39, 142.14, 145.05, 146.15, 155.66, 162.80; MS *m/z* %: 395.3 (M^+, 26.57); Anal. Calcd. for $C_{18}H_{17}N_7O_2S$: C, 54.67; H, 4.33; N, 24.79; found C, 55.01; H, 4.29; N, 24.88.

4.1.2.3. 4-((6-Amino-2-(4-fluorophenyl)-1*H*-imidazo[1,2-*b*]pyrazol-7-yl)diazenyl)benzenesulfonamide (**8c**)

Yield (40%); brick red powder; m.p. >300 °C; IR: 3417, 3305, 3217, 3174 (NH, $2NH_2$), 1323, 1153 (SO_2); ^{1}H NMR *δ ppm*: 7.39-7.41 (m, 4H, 2H, -SO_2NH_2 and 2H, Ar-H), 7.75 (br s, 2H, -NH_2 of pyrazole), 7.88 (d, 2H, Ar-H, *J* = 7.6 Hz), 7.97-8.05 (m, 4H, Ar-H), 8.47 (s, 1H, Ar-H), 11.95 (br s, 1H, -NH); ^{13}C NMR *δ ppm*: 111.39, 116.05, 116.81 ($^2J_{F-C}$ = 21 Hz), 119.12, 125.15, 127.65, 127.69 ($^3J_{F-C}$ = 8 Hz), 128.86, 135.33, 140.02, 145.36, 162.71, 162.79 ($^1J_{F-C}$ = 246 Hz); MS *m/z* %: 399.7 (M^+, 29.37); Anal. Calcd. for $C_{17}H_{14}FN_7O_2S$: C, 51.12; H, 3.53; N, 24.55; found C, 50.84; H, 3.48; N, 24.65.

4.1.2.4. 4-((6-Amino-2-(4-chlorophenyl)-1*H*-imidazo[1,2-*b*]pyrazol-7-yl)diazenyl)benzenesulfonamide (**8d**)

Yield (43%); brick red powder; m.p. >300 ◦C; IR: 3448, 3410, 3352, 3259, 3170 (NH, $2NH_2$), 1319, 1153 (SO_2); ^{1}H NMR *δ ppm*: 7.36 (br s, 2H, -SO_2NH_2), 7.60-7.74 (m, 4H, 2H, Ar-H and 2H, -NH_2 of pyrazole), 7.87 (d, 2H, Ar-H, *J* = 8.4 Hz), 7.95-8.00 (m, 4H, Ar-H), 8.48 (s, 1H, Ar-H), 11.89 (br s, 1H, -NH); MS *m/z* %: 417.8 (M^++2, 13.88), 415.8 (M^+, 39.41); Anal. Calcd. for $C_{17}H_{14}ClN_7O_2S$: C, 49.10; H, 3.39; N, 23.58; found C, 48.91; H, 3.41; N, 23.54.

4.1.2.5. 4-((6-Amino-2-(4-bromophenyl)-1*H*-imidazo[1,2-*b*]pyrazol-7-yl)diazenyl)benzenesulfonamide (**8e**)

Yield (40%); brick red powder; m.p. >300 ◦C; IR: 3344, 3255, 3167, 3086 (NH, $2NH_2$), 1330, 1153 (SO_2); ^{1}H NMR *δ ppm*: 7.36 (br s, 2H, -SO_2NH_2), 7.73-7.79 (m, 4H, 2H, Ar-H and 2H, -NH_2 of pyrazole), 7.87-7.91 (m, 4H, Ar-H), 7.99 (d, 2H, Ar-H, *J* = 8.0 Hz), 8.50 (s, 1H, Ar-H), 11.88 (br s, 1H, -NH); MS *m/z* %: 462.3 (M^++2, 34.01), 460.3 (M^+, 31.26); Anal. Calcd. for $C_{17}H_{14}BrN_7O_2S$: C, 44.36; H, 3.07; N, 21.30; found C, 44.65; H, 3.11; N, 21.20.

*4.1.3. Synthesis of4-((2-amino-7-(4-substitutedphenyl)pyrazolo[1,5-a]pyrimidin-3-yl)diazenyl)benzenesulfonamide (**9a-h**)*

A mixture of **4** (1.4 g, 0.005 mol) and **6a-h** (0.005mol) in glacial acetic acid (5 mL) was heated under reflux for 1h. The formed precipitate was filtered while hot, washed with cold ethanol and water, and recrystallized from dioxane to furnish target sulfonamides **9a-h**.

4.1.3.1. 4-((2-Amino-7-phenylpyrazolo[1,5-*a*]pyrimidin-3-yl)diazenyl)benzenesulfonamide (**9a**)

Yield (58%); yellow powder; m.p. 298-300 ◦C; IR: 3437, 3352, 3224, 3101 ($2NH_2$), 1300, 1149 (SO_2); ^{1}H NMR *δ ppm*: 7.31 (d, 1H, Ar-H, *J* = 4.8 Hz), 7.42-7.43 (m, 4H, 2H, -NH_2 and 2H, -SO_2NH_2), 7.60-7.63 (m, 3H, Ar-H), 7.95-8.00 (m, 4H, Ar-H), 8.07 (d, 2H, Ar-H, *J* = 8.0 Hz), 8.63 (d, 1H, Ar-H, *J* = 4.8 Hz); MS *m/z* %: 393.3 (M^+, 43.43); Anal. Calcd. for $C_{18}H_{15}N_7O_2S$: C, 54.95; H, 3.84; N, 24.92; found C, 55.16; H, 3.81; N, 24.84.

4.1.3.2. 4-((2-Amino-7-(4-methylphenyl)pyrazolo[1,5-*a*]pyrimidin-3-yl)diazenyl)benzenesulfonamide (**9b**)

Yield (69%); yellow powder; m.p. 297-299 ◦C; IR: 3417, 3255, 3186, 3143 ($2NH_2$), 1330, 1149 (SO_2); ^{1}H NMR *δ ppm*: 2.43 (s, 3H, CH_3), 7.32 (d, 1H, Ar-H, *J* = 4.8 Hz), 7.41-7.43 (m, 6H, 2H,

Ar-H, 2H, -NH_2 and 2H, -SO_2NH_2), 7.93-7.99 (m, 4H, Ar-H), 8.02 (d, 2H, Ar-H, *J* = 8.0 Hz), 8.62 (d, 1H, Ar-H, *J* = 4.8 Hz); ^{13}C NMR *δ ppm*: 21.57 (CH_3), 110.18, 116.13, 121.69, 127.32, 127.73, 129.50, 130.02, 141.82, 143.34, 145.89, 148.66, 151.40, 152.33, 155.41; HRMS (ESI) for $C_{19}H_{18}O_2N_7{}^{32}S$, calcd 408.12372, found 408.12357 $[M+H]^+$.

4.1.3.3. 4-((2-Amino-7-(4-fluorophenyl)pyrazolo[1,5-*a*]pyrimidin-3-yl)diazenyl)benzenesulfonamide (**9c**)

Yield (55%); yellow powder; m.p. >300 °C; IR: 3437, 3379, 3259, 3186 (2NH_2), 1334, 1149 (SO_2); ^{1}H NMR *δ ppm*: 7.32 (d, 1H, Ar-H, *J* = 4.8 Hz), 7.42-7.49 (m, 6H, 2H, Ar-H, 2H, -NH_2 and 2H, -SO_2NH_2), 7.94-8.00 (m, 4H, Ar-H), 8.17 (dd, 2H, Ar-H, *J* = 8.0 Hz, *J* = 4.0 Hz), 8.63 (d, 1H, Ar-H, *J* = 4.4 Hz); ^{13}C NMR *δ ppm*: 110.40, 116.04 ($^2J_{F-C}$ = 22 Hz), 121.72, 127.04, 127.33, 132.79 ($^3J_{F-C}$ = 9 Hz), 143.38, 144.84, 148.57, 151.43, 152.36, 155.37, 164.01 ($^1J_{F-C}$ = 248 Hz), 172.49; MS *m/z* %: 411.4 (M^+, 14.04); Anal. Calcd. for $C_{18}H_{14}FN_7O_2S$: C, 52.55; H, 3.43; N, 23.83; found C, 52.37; H, 3.49; N, 23.76.

4.1.3.4. 4-((2-Amino-7-(4-chlorophenyl)pyrazolo[1,5-*a*]pyrimidin-3-yl)diazenyl)benzenesulfonamide (**9d**)

Yield (64%); yellow powder; m.p. >300 °C; IR: 3417, 3336, 3259, 3186 (2NH_2), 1330, 1153 (SO_2); ^{1}H NMR *δ ppm*: 7.36 (d, 1H, Ar-H, *J* = 4.8 Hz), 7.40-7.42 (m, 4H, 2H, -NH_2 and 2H, -SO_2NH_2), 7.70 (d, 2H, Ar-H, *J* = 8.4 Hz), 7.93 (d, 2H, Ar-H, *J* = 8.0 Hz), 7.97 (d, 2H, Ar-H, *J* = 8.0 Hz), 8.13 (d, 2H, Ar-H, *J* = 8.8 Hz), 8.65 (d, 1H, Ar-H, *J* = 4.8 Hz); ^{13}C NMR *δ ppm*: 110.46, 116.12, 121.73, 127.33, 129.05, 129.46, 131.98, 136.43, 143.43, 144.67, 148.52, 151.50, 152.37, 155.35; HRMS (ESI) for $C_{18}H_{15}O_2N_7ClS$, calcd 428.06910, found 428.06914 $[M+H]^+$.

4.1.3.5. 4-((2-Amino-7-(4-bromophenyl)pyrazolo[1,5-*a*]pyrimidin-3-yl)diazenyl)benzenesulfonamide (**9e**)

Yield (61%); yellow powder; m.p. >300 °C; IR: 3417, 3340, 3255, 3186 (2NH_2), 1330, 1153 (SO_2); ^{1}H NMR *δ ppm*: 7.33 (d, 1H, Ar-H, *J* = 4.8 Hz), 7.42 (br s, 4H, 2H, -NH_2 and 2H, -SO_2NH_2), 7.82 (d, 2H, Ar-H, *J* = 8.4 Hz), 7.94-8.00 (m, 4H, Ar-H), 8.04 (d, 2H, Ar-H, *J* = 8.8 Hz), 8.64 (d, 1H, Ar-H, *J* = 4.4 Hz); MS *m/z* %: 474.2 (M^++2, 21.56), 472.2 (M^+, 20.94); Anal. Calcd. for $C_{18}H_{14}BrN_7O_2S$: C, 45.77; H, 2.99; N, 20.76; found C, 45.55; H, 2.97; N, 20.78.

4.1.3.6. 4-((2-Amino-7-(4-methoxyphenyl)pyrazolo[1,5-*a*]pyrimidin-3-yl)diazenyl)benzenesulfonamide (**9f**)

Yield (65%); yellow powder; m.p. >300 °C; IR: 3425, 3305, 3244, 3186 ($2NH_2$), 1327, 1149 (SO_2); ^{1}H NMR *δ ppm*: 3.87 (s, 3H, OCH_3), 7.13 (d, 2H, Ar-H, *J* = 8.8 Hz), 7.30 (d, 1H, Ar-H, *J* = 4.8 Hz), 7.43 (br s, 4H, 2H, -NH_2 and 2H, -SO_2NH_2), 7.94-7.99 (m, 4H, Ar-H), 8.15 (d, 2H, Ar-H, *J* = 8.8 Hz), 8.58 (d, 1H, Ar-H, *J* = 4.4 Hz); ^{13}C NMR *δ ppm*: 55.98 (OCH_3), 109.75, 114.36, 116.11, 121.68, 122.51, 127.32, 131.98, 143.27, 145.53, 148.76, 151.21, 152.29, 155.43, 162.01; MS *m/z* %: 423.3 (M^+, 15.67); Anal. Calcd. for $C_{19}H_{17}N_7O_3S$: C, 53.89; H, 4.05; N, 23.15; found C, 54.21; H, 4.12; N, 23.05.

4.1.3.7. 4-((2-Amino-7-(4-nitrophenyl)pyrazolo[1,5-*a*]pyrimidin-3-yl)diazenyl)benzenesulfonamide (**9g**)

Yield (63%); orange powder; m.p. >300 °C; IR : 3417, 3383, 3271, 3190 ($2NH_2$), 1330, 1149 (SO_2); ^{1}H NMR *δ ppm*: 7.41-7.45 (m, 5H, 1H, Ar-H, 2H, -NH_2 and 2H, -SO_2NH_2), 7.93 (d, 2H, Ar-H, *J* = 8.4 Hz), 7.98 (d, 2H, Ar-H, *J* = 8.8 Hz), 8.32 (d, 2H, Ar-H, *J* = 8.8 Hz), 8.44 (d, 2H, Ar-H, *J* = 8.8 Hz), 8.70 (d, 1H, Ar-H, *J* = 4.8 Hz); MS *m/z* %: 438.0 (M^+, 30.37); Anal. Calcd. for $C_{18}H_{14}N_8O_4S$: C, 49.31; H, 3.22; N, 25.56; found C, 49.71; H, 3.26; N, 25.65.

4.1.3.8. 4-((2-Amino-7-(thiophen-2-yl)pyrazolo[1,5-*a*]pyrimidin-3-yl)diazenyl)benzenesulfonamide (**9h**)

Yield (60%); orange powder; m.p. >300 °C; IR: 3417, 3321, 3236, 3116 ($2NH_2$), 1319, 1145 (SO_2); ^{1}H NMR *δ ppm*: 7.39-7.43 (m, 3H, 1H, Ar-H, 2H, -NH_2), 7.57 (s, 2H, -SO_2NH_2), 7.81 (d, 1H, Ar-H, *J* = 5.2 Hz), 7.95-8.00 (m, 4H, Ar-H), 8.17 (d, 1H, Ar-H, *J* = 4.4 Hz), 8.54-8.58 (m, 2H, Ar-H); MS *m/z* %: 399.4 (M^+, 13.60); Anal. Calcd. for $C_{16}H_{13}N_7O_2S_2$: C, 48.11; H, 3.28; N, 24.55; found C, 48.48; H, 3.24; N, 24.64.

*4.1.4. Synthesis of 4-((2,7-diamino-5-(4-substitutedphenyl)-6-cyanopyrazolo[1,5-a]pyrimidin-3-yl)diazenyl)benzenesulfonamide (**10a-e**)*

A suspension of the key intermediate **4** (1.4 g, 0.005 mol) in dry DMF (30 mL) was added to **7a-e** (0.005 mol), then heated under reflux for 8-10h. Then, the solvent was evaporated under vacuum and the residue was collected, washed with water, dried and crystallized from acetonitrile to afford the target sulfonamides **10a-e**.

4.1.4.1. 4-((2,7-Diamino-6-cyano-5-phenylpyrazolo[1,5-*a*]pyrimidin-3-yl)diazenyl)benzenesulfonamide (**10a**)

Yield (65%); yellow powder, m.p. 298-300 ◦C (reported m.p: 298 ^{0}C, [26]); IR: 3444, 3394, 3332, 3240, 3066 (3NH_2), 2214 (CN), 1361, 1149 (SO_2); ^{1}H NMR *δ ppm*: 7.25 (s, 2H, -NH_2), 7.44 (s, 2H, -SO_2NH_2), 7.60 (br s, 3H, Ar-H), 7.89-7.98 (m, 6H, Ar-H), 8.68 (br s, 2H, -NH_2); Anal. Calcd. for $C_{19}H_{15}N_9O_2S$: C, 52.65; H, 3.49; N, 29.08; found C, 53.00; H, 3.52; N, 29.18.

4.1.4.2. 4-((2,7-Diamino-5-(4-methylphenyl)-6-cyanopyrazolo[1,5-*a*]pyrimidin-3-yl)diazenyl)benzenesulfonamide (**10b**)

Yield (67%); yellow powder; m.p. 295-297 ◦C; IR: 3429, 3406, 3298, 3224, 3167, (3NH_2), 2222 (CN), 1334, 1153 (SO_2); ^{1}H NMR *δ ppm*: 2.43 (s, 3H, CH_3), 7.24 (s, 2H, -NH_2), 7.38-7.43 (m, 4H, 2H, Ar-H, 2H, -SO_2NH_2), 7.80 (d, 2H, Ar-H, *J* = 8.0 Hz), 7.95 (br s, 4H, Ar-H), 8.64 (br s, 2H, -NH_2); ^{13}C NMR *δ ppm*: 21.48 (CH_3), 116.53, 117.90, 121.88, 127.33, 129.13, 129.37, 134.76, 140.81, 143.70, 147.13, 149.38, 152.52, 155.11, 161.79, 162.79; MS *m/z* %: 447.66 (M^+, 57.3); Anal. Calcd. for $C_{20}H_{17}N_9O_2S$: C, 53.68; H, 3.83; N, 28.17; found C, 53.98; H, 3.77; N, 28.27.

4.1.4.3. 4-((2,7-Diamino-5-(4-fluorophenyl)-6-cyanopyrazolo[1,5-*a*]pyrimidin-3-yl)diazenyl)benzenesulfonamide (**10c**)

Yield (59%); yellow powder; m.p. >300 ◦C; IR: 3444, 3332, 3236 (3NH_2), 2214 (CN), 1338, 1149 (SO_2); ^{1}H NMR *δ ppm*: 7.24 (s, 2H, -NH_2), 7.41 (s, 2H, -SO_2NH_2), 7.94-7.97 (m, 8H, Ar-H), 8.68 (br s, 2H, -NH_2); HRMS (ESI) for $C_{19}H_{15}O_2N_9F^{32}S$, calcd 452.10480, found 452.10482 $[M+H]^+$.

4.1.4.4. 4-((2,7-Diamino-5-(4-chlorophenyl)-6-cyanopyrazolo[1,5-*a*]pyrimidin-3-yl)diazenyl)benzenesulfonamide (**10d**)

Yield (63 %); yellow powder; m.p. >300 ◦C (reported m.p: >300^{0}C [26]); IR: 3433, 3406, 3352, 3298, 3228, 3174 (3NH_2), 2222 (CN), 1338, 1153 (SO_2); ^{1}H NMR *δ ppm*: 7.25 (s, 2H, -NH_2), 7.44 (s, 2H, -SO_2NH_2), 7.65 (d, 2H, Ar-H, *J* = 8.4 Hz), 7.91-7.96 (m, 6H, Ar-H), 8.71 (br s, 2H, -NH_2); ^{13}C NMR *δ ppm*: 116.32, 117.95, 121.92, 127.33, 128.95, 131.03, 135.74, 136.36, 143.79, 147.94, 149.28, 152.54, 155.06, 160.59, 162.79; MS *m/z* %: 469.20 (M^++2, 17.85), 467.2 (M^+, 55.65); Anal. Calcd. for $C_{19}H_{14}ClN_9O_2S$: C, 48.77; H, 3.02; N, 26.94; found C, 49.11; H, 2.96; N, 26.86.

4.1.4.5. 4-((2,7-Diamino-5-(4-bromophenyl)-6-cyanopyrazolo[1,5-*a*]pyrimidin-3-yl)diazenyl)benzenesulfonamide (**10e**)

Yield (61%); yellow powder; m.p. >300 °C; IR: 3483, 3425, 3340, 3298, 3244, 3182 ($3NH_2$), 2210 (CN), 1327, 1149 (SO_2); ^{1}H NMR δ *ppm*: 7.25 (s, 2H, -NH_2), 7.44 (s, 2H, -SO_2NH_2), 7.79-7.96 (m, 4H, Ar-H), 7.96 (br s, 4H, Ar-H), 8.69 (br s, 2H, -NH_2); MS *m/z* %: 514.1 (M^++2, 16.98), 512.1 (M^+, 15.66); Anal. Calcd. for $C_{19}H_{14}BrN_9O_2S$: C, 44.54; H, 2.75; N, 24.61; found C, 44.57; H, 2.78; N, 24.54.

4.2 Biological evaluation

4.2.1. CA inhibitory assay

An Applied Photophysics stopped-flow instrument has been used for assaying the CA catalysed CO_2 hydration activity, as reported earlier. [32, 40-42] The inhibition constants were obtained by non-linear least-squares methods using PRISM 3 and the Cheng-Prusoff equation as reported earlier [18], and represent the mean from at least three different determinations. The four tested CA isofoms were recombinant ones obtained in-house as reported earlier [23].

4.2.2. CDK inhibition assays

The assays were performed as described earlier [43, 44]. Briefly, CDK2/cyclin E kinase was produced via baculoviral infection in Sf9 cells, CDK9/Cyclin T1 was purchased from ProQinase. The kinases were assayed with histone H1 (for CDK2) or $(YSPTSPS)_2KK$ (for CDK9) in the presence of 15 or 1.5 µM ATP (for CDK2 and CDK9, respectively), 0.05 µCi [γ-^{33}P]ATP and of the test compound in a final volume of 10 µL, all in a reaction buffer (60 mM HEPES-NaOH, pH 7.5, 3 mM $MgCl_2$, 3 mM $MnCl_2$, 3 µM Na-orthovanadate, 1.2 mM DTT, 2.5 µg / 50 µl $PEG_{20.000}$). The reactions were stopped by adding 5 µL of 3 % aq. H_3PO_4. Aliquots were spotted onto P-81 phosphocellulose (Whatman), washed 3× with 0.5 % aq. H_3PO_4 and finally air-dried. Kinase inhibition was quantified using a FLA-7000 digital image analyzer (Fujifilm).

4.2.3. In Vitro Antitumor screening against 60 cancer cell lines

The antitumor assay was performed according to the protocol of the Drug Evaluation Branch, NCI, Bethesda [45]. A 48 h drug exposure protocol was adopted, and sulforhodamine B (SRB) assay [33] was utilized to assess the cell growth and viability, as reported earlier [46, 47].

4.2.4. Antiproliferative activity against MCF-7 and MDA-MB-468 cell lines

Breast cancer MCF-7 and MDA-MB-468 cell lines were obtained from American Type Culture Collection (ATCC). Both cells were grown in DMEM. The cells were supplemented with 10% heat-inactivated fetal bovine serum, 1% L-glutamine (2.5 mM), HEPES buffer (10 mM), 50 μg/mL gentamycin. All cells were maintained at 37 C in a humidified atmosphere with 5% CO_2. Cytotoxicity was determined following the MTT assay, as reported earlier [48, 49].

4.2.5. Cell Cycle Analysis

MCF-7 cells were treated with sulfonamides **10a**, **10c** and **10d** for 24 hour at their IC_{50} concentration, and then cells were washed twice with ice-cold phosphate buffered saline (PBS). Subsequently, the treated cells were collected by centrifugation, fixed in ice-cold 70% (*v*/*v*) ethanol, washed with PBS, re-suspended with 100 μg/mL RNase, stained with 40 μg/mL PI, and analyzed by flow cytometry using FACS Calibur (Becton Dickinson, BD, USA). The cell cycle distributions were calculated using CellQuest software 5.1 (Becton Dickinson) [50, 51].

4.2.6. Annexin V-FITC Apoptosis Assay

Phosphatidylserine externalization was assayed using Annexin V-FITC/PI apoptosis detection kit (BD Biosciences, USA) according to the manufacturer's instructions, as reported earlier [47, 52].

4.2.7. Computational studies

The crystal structure of hCA II (PDB 5LJT) [37], hCA IX (PDB 5FL4) [38] and XII (pdb JLD0 [39]) were prepared using the Protein Preparation Wizard tool implemented in Maestro - Schrödinger suite, assigning bond orders, adding hydrogens, deleting water molecules, and optimizing H-bonding networks. Energy minimization protocol with a root mean square deviation (RMSD) value of 0.30 was applied using an Optimized Potentials for Liquid Simulation (OPLS3e) force field. 3D ligand structures were prepared by Maestro [4a] and evaluated for their ionization states at pH 7.4 ± 0.5 with Epik [4b]. OPLS3e force field in Macromodel [4e] was used for energy minimization for a maximum number of 2500 conjugate gradient iteration and setting a convergence criterion of 0.05 kcal $mol^{-1}Å^{-1}$. The docking grid was centred on the center of mass of the co-crystallized ligands and Glide used with default settings.

Ligands were docked with the standard precision mode (SP) of Glide [4f] and the best 5 poses of each molecule retained as output. The best pose for each compound, evaluated in terms of coordination, hydrogen bond interactions and hydrophobic contacts, was refined with Prime [4d] with a VSGB solvation model considering the target flexible within 3Å around the ligand [53-55]

Acknowledgments

This research was supported by the Czech Science Foundation (19-09086S), the European Regional Development Fund (Project ENOCH, No. CZ.02.1.01/0.0/0.0/16_019/0000868) and Palacky University (IGA_PrF_2019_013).

References

[1] C. Fernández-López, J. Expósito-Hernández, J.P. Arrebola-Moreno, M.Á. Calleja-Hernández, M. Expósito-Ruíz, R. Guerrero-Tejada, I. Linares, J. Cabeza-Barrera, Trends in phase III randomized controlled clinical trials on the treatment of advanced non-small-cell lung cancer, Cancer. Med-US, 5 (2016) 2190-2197.

[2] W.H. Organization, World health statistics 2016: monitoring health for the SDGs sustainable development goals, W. H. O, 2016.

[3] A. Angeli, C.T. Supuran, Therapeutic Use of Carbonic Anhydrase Inhibitors and Their Multiple Drug Interactions, Pharmaceutical Biocatalysis: Fundamentals, Enzyme Inhibitors, and Enzymes in Health and Diseases, (2019) 73.

[4] L. Vats, R. Kumar, S. Bua, A. Nocentini, P. Gratteri, C.T. Supuran, P.K. Sharma, Continued exploration and tail approach synthesis of benzenesulfonamides containing triazole and dual triazole moieties as carbonic anhydrase I, II, IV and IX inhibitors, Eur. J. Med. Chem, 183 (2019) 111698.

[5] M.Y. Mboge, R. McKenna, S.C. Frost, Advances in anti-cancer drug development targeting Carbonic Anhydrase IX and XII, Topics in Anticancer Res, 5 (2015) 3.

[6] C.T. Supuran, V. Alterio, A. Di Fiore, K. D'Ambrosio, F. Carta, S.M. Monti, G. De Simone, Inhibition of carbonic anhydrase IX targets primary tumors, metastases, and cancer stem cells: three for the price of one, Med. Res. Rev, 38 (2018) 1799-1836.

[7] S. Figel, R.A. Fenstermaker, Cell-cycle regulation, in: Handbook of Brain Tumor Chemotherapy, Molecular Therapeutics, and Immunotherapy, Elsevier, 2018, pp. 257-269.

[8] D.D. Fang, R. Tao, Q. Tang, S. Gu, G. Zhai, J. Li, Q. Wang, X. Fang, N. Li, D. Yang, Synergistic effect of BCL-2 inhibitor APG-2575 and CDK9 inhibitor in acute myeloid leukemia and DLBCL preclinical tumor models, in, AACR, 2019.

[9] V. Kryštof, P. Cankař, I. Fryšová, J. Slouka, G. Kontopidis, P. Džubák, M. Hajdúch, J. Srovnal, W.F. de Azevedo, M. Orság, 4-Arylazo-3, 5-diamino-1 H-pyrazole CDK inhibitors: SAR study, crystal structure in complex with CDK2, selectivity, and cellular effects, J. Med. Chem, 49 (2006) 6500-6509.

[10] Y. Niu, J. Xu, T. Sun, Cyclin-Dependent Kinases 4/6 Inhibitors in Breast Cancer: Current Status, Resistance, and Combination Strategies, J. Cancer, 10 (2019) 5504.

[11] C. Sánchez-Martínez, M.J. Lallena, S.G. Sanfeliciano, A. de Dios, Cyclin Dependent Kinase (CDK) inhibitors as anticancer drugs: Recent Advances (2015-2019), Bioorg. Med. Chem. Lett, (2019) 126637.

[12] K. El Hage, J.-P. Piquemal, N. Oumata, L. Meijer, H. Galons, N. Gresh, A Simple Isomerization of the Purine Scaffold of a Kinase Inhibitor, Roscovitine, Affords a Four-to Seven-Fold Enhancement of Its Affinity for Four CDKs. Could This Be Traced Back to Conjugation-Induced Stiffenings/Loosenings of Rotational Barriers?, ACS omega, 2 (2017) 3467-3474.

[13] J. Cicenas, K. Kalyan, A. Sorokinas, E. Stankunas, J. Levy, I. Meskinyte, V. Stankevicius, A. Kaupinis, M. Valius, Roscovitine in cancer and other diseases, Ann. Transl. Med, 3 (2015).

[14] S.S.A. El-Karim, Y.M. Syam, A.M. El Kerdawy, T.M. Abdelghany, New thiazol-hydrazono-coumarin hybrids targeting human cervical cancer cells: Synthesis, CDK2 inhibition, QSAR and molecular docking studies, Bioorg. Chem, 86 (2019) 80-96.

[15] C.R. Coxon, E. Anscombe, S.J. Harnor, M.P. Martin, B. Carbain, B.T. Golding, I.R. Hardcastle, L.K. Harlow, S. Korolchuk, C.J. Matheson, Cyclin-dependent kinase (CDK) inhibitors: structure–activity relationships and insights into the CDK-2 selectivity of 6-substituted 2-arylaminopurines, J. Med. Chem, 60 (2017) 1746-1767.

[16] R. Jorda, J. Navrátilová, Z. Hušková, E. Schütznerová, P. Cankař, M. Strnad, V. Kryštof, Arylazopyrazole AAP 1742 Inhibits CDK s and Induces Apoptosis in Multiple Myeloma Cells via Mcl-1 Downregulation, Chem. Biol. Drug Des, 84 (2014) 402-408.

[17] R. Jorda, E. Schütznerová, P. Cankař, V. Brychtová, J. Navrátilová, V. Kryštof, Novel arylazopyrazole inhibitors of cyclin-dependent kinases, Bioorg. Med. Chem, 23 (2015) 1975-1981.

[18] W.M. Eldehna, M.F. Abo-Ashour, A. Nocentini, R.S. El-Haggar, S. Bua, A. Bonardi, S.T. Al-Rashood, G.S. Hassan, P. Gratteri, H.A. Abdel-Aziz, Enhancement of the tail hydrophobic interactions within the carbonic anhydrase IX active site via structural extension: Design and synthesis of novel N-substituted isatins-SLC-0111 hybrids as carbonic anhydrase inhibitors and antitumor agents, Eur. J. Med. Chem, 162 (2019) 147-160.

[19] W.M. Eldehna, M.A. Abdelrahman, A. Nocentini, S. Bua, S.T. Al-Rashood, G.S. Hassan, A. Bonardi, A.A. Almehizia, H.M. Alkahtani, A. Alharbi, Synthesis, biological evaluation and in silico studies with 4-benzylidene-2-phenyl-5 (4H)-imidazolone-based benzenesulfonamides as novel selective carbonic anhydrase IX inhibitors endowed with anticancer activity, Bioorg. Chem, 90 (2019) 103102.

[20] M.A. Abdelrahman, W.M. Eldehna, A. Nocentini, S. Bua, S.T. Al-Rashood, G.S. Hassan, A. Bonardi, A.A. Almehizia, H.M. Alkahtani, A. Alharbi, Novel Diamide-Based Benzenesulfonamides as Selective Carbonic Anhydrase IX Inhibitors Endowed with Antitumor Activity: Synthesis, Biological Evaluation and In Silico Insights, , Int. J. Mol. Sci, 20 (2019) 2484.

[21] M.F. Abo-Ashour, W.M. Eldehna, A. Nocentini, A. Bonardi, S. Bua, H.S. Ibrahim, M.M. Elaasser, V. Kryštof, R. Jorda, P. Gratteri, 3-Hydrazinoisatin-based benzenesulfonamides as novel carbonic anhydrase inhibitors endowed with anticancer activity: Synthesis, in vitro biological evaluation and in silico insights, Eur. J. Med. Chem, (2019) 111768.

[22] A.M. Alafeefy, R. Ahmad, M. Abdulla, W.M. Eldehna, A.-M.S. Al-Tamimi, H.A. Abdel-Aziz, O. Al-Obaid, F. Carta, A.A. Al-Kahtani, C.T. Supuran, Development of certain new 2-substituted-quinazolin-4-yl-aminobenzenesulfonamide as potential antitumor agents, Eur. J. Med. Chem, 109 (2016) 247-253.

[23] W.M. Eldehna, A. Nocentini, S.T. Al-Rashood, G.S. Hassan, H.M. Alkahtani, A.A. Almehizia, A.M. Reda, H.A. Abdel-Aziz, C.T. Supuran, Tumor-associated carbonic anhydrase isoform IX and XII inhibitory properties of certain isatin-bearing sulfonamides endowed with in vitro antitumor activity towards colon cancer, Bioorg. Chem, 81 (2018) 425-432.

[24] A.Z.A.E.-B. Hassanien, I.S.A. Hafiz, M.H. Elnagdi, Utility of [(p-sulfonamidophenyl) azo] malononitrile in the synthesis of polyfunctionally substituted pyrimidine, pyrazole, isoxazole and pyridazine derivatives, J. Chem. Res, 23 (1999) 8-9.

[25] M.A. Abdelgawad, M.B. Labib, M. Abdel-Latif, Pyrazole-hydrazone derivatives as anti-inflammatory agents: Design, synthesis, biological evaluation, COX-1, 2/5-LOX inhibition and docking study, Bioorg. Chem, 74 (2017) 212-220.

[26] A. Hassanien, A. Amr, S. Ghozlan, Utility of (p-Sulfonamidophenyl) azomalononitrile, and Ethyl Acetoacetate in Synthesis of Fused Azole and Azines Derivatives II, J. Chin. Chem. Soc-Taip, 47 (2000) 1273-1278.

[27] L.C. King, G.K. Ostrum, Selective Bromination with copper (II) bromide1, J. Org. Chem, 29 (1964) 3459-3461.

[28] W. Gao, H. Lv, X. Zhang, Rh/DuanPhos-Catalyzed Asymmetric Hydrogenation of β-Acetylamino Vinylsulfides: An Approach to Chiral β-Acetylamino Sulfides, Org. lett, 19 (2017) 2877-2880.

[29] F. Arioli, S. Borrelli, F. Colombo, F. Falchi, I. Filippi, E. Crespan, A. Naldini, G. Scalia, A. Silvani, G. Maga, N-[2-Methyl-5-(triazol-1-yl) phenyl] pyrimidin-2-amine as a Scaffold for the Synthesis of Inhibitors of Bcr-Abl, Chem.Med.Chem, 6 (2011) 2009-2018.

[30] M.A. Al-Shiekh, H.Y. Medrassi, M.H. Elnagdi, E.A. Hafez, Studies with 2-arylhydrazono-3-oxopropanals: Routes for the synthesis of pyridazine-3, 4-dicarboxylate and 3, 5-diaroylpyrazoles, Arkivoc, 17 (2008) 36-47.

[31] L.C. Chang, J.K. von Frijtag Drabbe Künzel, T. Mulder-Krieger, R.F. Spanjersberg, S.F. Roerink, G. van den Hout, M.W. Beukers, J. Brussee, A.P. IJzerman, A series of ligands displaying a remarkable agonistic− antagonistic profile at the adenosine A1 receptor, J. Med. Chem, 48 (2005) 2045-2053.

[32] R.G. Khalifah, The carbon dioxide hydration activity of carbonic anhydrase I. Stop-flow kinetic studies on the native human isoenzymes B and C, J. Biol. Chem, 246 (1971) 2561-2573.

[33] P. Skehan, R. Storeng, D. Scudiero, A. Monks, J. McMahon, D. Vistica, J.T. Warren, H. Bokesch, S. Kenney, M.R. Boyd, New colorimetric cytotoxicity assay for anticancer-drug screening, JNCI: J. Natl. Cancer Inst, 82 (1990) 1107-1112.

[34] C. Trastour, E. Benizri, F. Ettore, A. Ramaioli, E. Chamorey, J. Pouysségur, E. Berra, HIF-1α and CA IX staining in invasive breast carcinomas: Prognosis and treatment outcome, , Int. J. Cancer, 120 (2007) 1451-1458.

[35] T. Mosmann, Rapid colorimetric assay for cellular growth and survival: application to proliferation and cytotoxicity assays, J. Immunol. Methods, 65 (1983) 55-63.

[36] N.K. Tafreshi, M.C. Lloyd, J.B. Proemsey, M.M. Bui, J. Kim, R.J. Gillies, D.L. Morse, Evaluation of CAIX and CAXII Expression in Breast Cancer at Varied O 2 Levels: CAIX is the Superior Surrogate Imaging Biomarker of Tumor Hypoxia, Mol. Imaging. Biol, 18 (2016) 219-231.

[37] A. Nocentini, M. Ferraroni, F. Carta, M. Ceruso, P. Gratteri, C. Lanzi, E. Masini, C.T. Supuran, Benzenesulfonamides incorporating flexible triazole moieties are highly effective carbonic anhydrase inhibitors: synthesis and kinetic, crystallographic, computational, and intraocular pressure lowering investigations, J. Med. Chem, 59 (2016) 10692-10704.

[38] J. Leitans, A. Kazaks, A. Balode, J. Ivanova, R. Zalubovskis, C.T. Supuran, K. Tars, Efficient expression and crystallization system of cancer-associated carbonic anhydrase isoform IX, J. Med. Chem, 58 (2015) 9004-9009.

[39] D.A. Whittington, A. Waheed, B. Ulmasov, G.N. Shah, J.H. Grubb, W.S. Sly, D.W. Christianson, Crystal structure of the dimeric extracellular domain of human carbonic anhydrase XII, a bitopic membrane protein overexpressed in certain cancer tumor cells, Proc. Natl. Acad. Sci. U.S.A, 98 (2001) 9545-9550.

[40] A. Nocentini, M. Ceruso, S. Bua, C.L. Lomelino, J.T. Andring, R. McKenna, C. Lanzi, S. Sgambellone, R. Pecori, R. Matucci, Discovery of β-Adrenergic Receptors Blocker–Carbonic Anhydrase Inhibitor Hybrids for Multitargeted Antiglaucoma Therapy, J. Med. Chem, 61 (2018) 5380-5394.

[41] M.F. Abo-Ashour, W.M. Eldehna, A. Nocentini, H.S. Ibrahim, S. Bua, S.M. Abou-Seri, C.T. Supuran, Novel hydrazido benzenesulfonamides-isatin conjugates: Synthesis, carbonic anhydrase inhibitory activity and molecular modeling studies, Eur. J. Med. Chem. 157 (2018) 28-36.

[42] b) M.M. Al-Sanea, A. Elkamhawy, S. Paik, S. Bua, S.H. Lee, M.A. Abdelgawad, E.J. Roh, W.M. Eldehna, C.T. Supuran, Synthesis and biological evaluation of novel 3-(quinolin-4-

ylamino)benzenesulfonamides as carbonic anhydrase isoforms I and II inhibitors, J. Enzym. Inhib. Med. Chem. 34 (2019) 1457–1464.

[43] T. Gucky, R. Jorda, M. Zatloukal, V.c. Bazgier, K. Berka, E. Řezníčková, T. Béres, M. Strnad, V. Kryštof, A novel series of highly potent 2, 6, 9-trisubstituted purine cyclin-dependent kinase inhibitors, J. Med. Chem, 56 (2013) 6234-6247.

[44] M. Zatloukal, R. Jorda, T. Gucký, E. Řezníčková, J. Voller, T. Pospíšil, V. Malínková, H. Adamcová, V. Kryštof, M. Strnad, Synthesis and in vitro biological evaluation of 2, 6, 9-trisubstituted purines targeting multiple cyclin-dependent kinases, Eur. J. Med. Chem, 61 (2013) 61-72.

[45] B.A. Teicher, Anticancer drug development guide: preclinical screening, clinical trials, and approval, Springer Science & Business Media, 2013.

[46] a) W.M. Eldehna, G.S. Hassan, S.T. Al-Rashood, T. Al-Warhi, A.E. Altyar, H.M. Alkahtani, A.A. Almehizia, H.A. Abdel-Aziz, Synthesis and in vitro anticancer activity of certain novel 1-(2-methyl-6-arylpyridin-3-yl)-3-phenylureas as apoptosis-inducing agents, J. Enzym. Inhib. Med. Chem, 34 (2019) 322-332, b) W.M. Eldehna, M. Fares, H.S. Ibrahim, M.A. Alsherbiny, M.H. Aly, H.A. Ghabbour and H.A. Abdel-Aziz, Synthesis and Cytotoxic Activity of Biphenylurea Derivatives Containing Indolin-2-one Moieties, Molecules, 21 (2016), p.762.

[47] W.M. Eldehna, M.F. Abo-Ashour, H.S. Ibrahim, G.H. Al-Ansary, H.A. Ghabbour, M.M. Elaasser, H.Y. Ahmed, N.A. Safwat, Novel [(3-indolylmethylene) hydrazono] indolin-2-ones as apoptotic anti-proliferative agents: design, synthesis and in vitro biological evaluation, J. Enzym. Inhib. Med. Chem, 33 (2018) 686-700.

[48] R.S. Ismail, S.M. Abou-Seri, W.M. Eldehna, N.S. Ismail, S.M. Elgazwi, H.A. Ghabbour, M.S. Ahmed, F.T. Halaweish, D.A.A. El Ella, Novel series of 6-(2-substitutedacetamido)-4-anilinoquinazolines as EGFR-ERK signal transduction inhibitors in MCF-7 breast cancer cells, Eur. J. Med. Chem emistry, 155 (2018) 782-796.

[49] H. Almahli, E. Hadchity, M.Y. Jaballah, R. Daher, H.A. Ghabbour, M.M. Kabil, N.S. Al-shakliah, W.M. Eldehna, Development of novel synthesized phthalazinone-based PARP-1 inhibitors with apoptosis inducing mechanism in lung cancer, Bioorg. Chem, 77 (2018) 443-456.

[50] W.M. Eldehna, D.H. EL-Naggar, A.R. Hamed, H.S. Ibrahim, H.A. Ghabbour, H.A. Abdel-Aziz, One-pot three-component synthesis of novel spirooxindoles with potential cytotoxic

activity against triple-negative breast cancer MDA-MB-231 cells, Journal of enzyme inhibition and medicinal chemistry, 33 (2018) 309-318.

[51] A. Sabt, O.M. Abdelhafez, R.S. El-Haggar, H.M. Madkour, W.M. Eldehna, E.E.-D.A. El-Khrisy, M.A. Abdel-Rahman, L.A. Rashed, Novel coumarin-6-sulfonamides as apoptotic anti-proliferative agents: synthesis, in vitro biological evaluation, and QSAR studies, J. Enzym. Inhib. Med. Chem, 33 (2018) 1095-1107.

[52] W.M. Eldehna, H. Almahli, G.H. Al-Ansary, H.A. Ghabbour, M.H. Aly, O.E. Ismael, A. Al-Dhfyan, H.A. Abdel-Aziz, Synthesis and in vitro anti-proliferative activity of some novel isatins conjugated with quinazoline/phthalazine hydrazines against triple-negative breast cancer MDA-MB-231 cells as apoptosis-inducing agents, J. Enzym. Inhib. Med. Chem, 32 (2017) 600-613.

[53] A. Nocentini, P. Gratteri, C.T. Supuran, Phosphorus versus Sulfur: Discovery of Benzenephosphonamidates as Versatile Sulfonamide-Mimic Chemotypes Acting as Carbonic Anhydrase Inhibitors, Chem. Eur. J, 25 (2019) 1188-1192.

[54] A. Nocentini, A. Bonardi, P. Gratteri, B. Cerra, A. Gioiello, C.T. Supuran, Steroids interfere with human carbonic anhydrase activity by using alternative binding mechanisms, J. Enzym. Inhib. Med. Chem, 33 (2018) 1453-1459.

[55] A. Nocentini, F. Carta, M. Tanc, S. Selleri, C.T. Supuran, C. Bazzicalupi, P. Gratteri, Deciphering the mechanism of human carbonic anhydrases inhibition with sulfocoumarins: computational and experimental studies, Chem. Eur. J, 24 (2018) 7840-7844.

Highlights

- New series of CAN508 sulfonamide-based analogues were synthesized.

- Inhibitory activities of all derivatives were evaluated toward hCA I, II, IX and XII isoforms.

- hCA IX and XII were efficiently inhibited with K_Is range of 6–67.6 and 10.1–88.6 nM.

- Pyrazolopyrimidines **9d, 9e and 10b** were found to be the most potent CDK2 inhibitors.

- Molecular docking was done to examine binding mode for the selective CAIX & XII inhibitors.

Declaration of Interest Statement

Conflicts of Interest: The authors have declared no conflict of interest.